

1 A Sturmian approach to photoionization of
2 molecules

3 C. M. Granados-Castro^{*a,b}, L. U. Ancarani^{†a}, G. Gasaneo^{b,c}, and
4 D. M. Mitnik^{c,d}

5 ^aEquipe TMS, UMR CNRS 7565, ICPM, Université de Lorraine,
6 57078 Metz, France

7 ^bDepartamento de Física, Universidad Nacional del Sur, 8000
8 Bahía Blanca, Buenos Aires, Argentina

9 ^cConsejo Nacional de Investigaciones Científicas y Técnicas
10 CONICET, Argentina

11 ^dInstituto de Astronomía y Física del Espacio (IAFE) and
12 Departamento de Física, Universidad de Buenos Aires, C1428EGA
13 Buenos Aires, Argentina

14 **Abstract**

15 An accurate theoretical description of photoionization processes is nec-
16 essary in order to understand a great variety of physical and chemical
17 phenomena, and allows one to test correlation effects of the target. Com-
18 pared to the case of many-electron atoms several extra challenges occur
19 for molecules. The scattering problem is generally multicenter and highly
20 non-central. Additionally, the molecular orientation with respect to the
21 polarization of the radiation field has to be taken into account. These
22 features make the computational task much more cumbersome and ex-
23 pensive than for atomic targets. In order to calculate cross sections one
24 needs to describe the ejected electron with a continuum wavefunction with
25 appropriate Coulomb asymptotic conditions. Making a number of initial
26 approximations, many different theoretical/numerical methods have been
27 proposed over the years. However, depending on the complexity of the
28 molecule, agreement among them is not uniform, and many features of the
29 experimental data are not so well reproduced. This is illustrated through
30 a number of examples. In order to have a global theoretical overview we
31 present a survey of most of the methods available in the literature, indicat-
32 ing their application to different molecules. Within a Born–Oppenheimer,
33 one-center expansion and single active electron approximation, we then
34 introduce a Sturmian approach to describe photoionization of molecular
35 targets. The method is based on the use of generalized Sturmian func-
36 tions for which correct boundary conditions can be chosen. This property
37 makes the method computationally efficient, as illustrated with results for
38 H₂O, NH₃ and CH₄.

39 **keywords:** Photoionization molecules; Theoretical methods; Generalized Stur-
40 mian functions; Cross sections

*carlos.mario-granados.castro@univ-lorraine.fr

†ugo.ancarani@univ-lorraine.fr

41 **Contents**

| | | |
|----|--|-----------|
| 42 | 1 Introduction | 4 |
| 43 | 2 Generalities | 5 |
| 44 | 3 Examples Taken from the Literature | 7 |
| 45 | 3.1 Molecular Hydrogen | 7 |
| 46 | 3.2 Molecular Nitrogen | 8 |
| 47 | 3.3 Carbon Dioxide | 9 |
| 48 | 3.4 Benzene | 9 |
| 49 | 4 Survey of Theoretical Methods | 10 |
| 50 | 4.1 CI | 10 |
| 51 | 4.2 Hartree–Fock Methods | 11 |
| 52 | 4.2.1 Self-Consistent Field | 11 |
| 53 | 4.2.2 Multiconfiguration time-dependent Hartree–Fock | 11 |
| 54 | 4.3 Density Functional Theory | 11 |
| 55 | 4.3.1 Kohn–Sham DFT | 11 |
| 56 | 4.3.2 Time-Dependent DFT | 12 |
| 57 | 4.4 Complex Methods | 12 |
| 58 | 4.4.1 Complex Scaling | 12 |
| 59 | 4.4.2 Complex Basis Functions | 13 |
| 60 | 4.5 Linear Algebraic Method | 13 |
| 61 | 4.6 Multi-Scattering | 14 |
| 62 | 4.7 Plane-Wave-Based Methods | 14 |
| 63 | 4.7.1 Plane-Wave Approximations | 14 |
| 64 | 4.7.2 Ground Inversion Potential Method | 15 |
| 65 | 4.8 <i>R</i> -Matrix Method | 15 |
| 66 | 4.9 Random Phase Approximation | 16 |
| 67 | 4.10 Stieltjes–Tchebycheff Technique | 16 |
| 68 | 4.11 The Kohn Variational Method | 17 |
| 69 | 4.11.1 Logarithmic Derivative Kohn Method | 18 |
| 70 | 4.11.2 Complex Kohn method | 18 |
| 71 | 4.12 The Schwinger Variational Method | 18 |
| 72 | 4.12.1 Iterative Schwinger | 19 |
| 73 | 4.12.2 Continued Fractions | 19 |
| 74 | 4.13 Crank–Nicolson | 20 |
| 75 | 5 Sturmian Approach | 20 |
| 76 | 5.1 Generalized Sturmian Functions | 20 |
| 77 | 5.2 Sturmian Approach to Photoionization Process | 21 |
| 78 | 5.2.1 Molecular Model Potentials | 21 |
| 79 | 5.2.2 Driven Equation and Cross Section | 22 |
| 80 | 5.2.3 Example: Hydrogen Atom | 25 |
| 81 | 5.3 Results For Molecules | 26 |
| 82 | 5.3.1 Water | 27 |
| 83 | 5.3.2 Ammonia | 27 |
| 84 | 5.3.3 Methane | 28 |

| | | |
|----|---|-----------|
| 85 | 6 Conclusions | 31 |
| 86 | A List of Photoionization Calculations for Different Molecules | 33 |
| 87 | Bibliography | 34 |

1 Introduction

The quantum description of both bound and unbound orbitals are necessary ingredients to study collisions with atoms and molecules. The study of single photoionization (PI) provides an indirect tool to test our capacity to describe correctly the target before and after the interaction, and thus correlation and many-body effects. PI plays an important role beyond atomic and molecular physics, since it has a wide variety of applications, such as astrophysics¹⁻³, planetary⁴⁻⁶, atmospheric^{7,8}, plasma⁹⁻¹¹ or medical physics^{12,13}. Also PI helps to understand different processes in surfaces, as structural changes upon surface adsorption, quantifying the relationship between shape resonances and the bond lengths¹⁴⁻¹⁷; or to characterize the relation between gas, chemisorbed and solid-state phases in surface reactions¹⁸⁻²¹.

In the last few years, a Sturmian approach^{22,23} has been introduced to study single and double ionization of atoms induced by electron or photon impact²⁴. It is the purpose of this contribution to extend, implement and apply such an approach to the PI of molecular targets. The Hamiltonian for molecules being generally multicenter and highly non-central makes life harder than in the case of atomic targets. Indeed, the absence of any spherical symmetry couples different angular momenta from different atomic orbitals (AOs) that conform the molecular orbitals (MOs), and thus convergence of “traditional” methods is considerably more difficult to achieve. Additionally, there are various many-body effects that can be important in ionization processes, such as the relaxation of all MOs, due to the creation of a hole (ionized electron), or the change of the remaining pair correlation energies because of such relaxation. An issue which does not arise in PI of atoms is the orientation of the molecular target. In most experiments the molecule is randomly oriented and this must be taken into account within the theoretical calculations.

When leaving an atomic or molecular target, an ionized electron needs to be described accurately by a continuum wavefunction, which has a well defined boundary conditions. Over the years, quite a few methods have been proposed and applied successfully to atoms. The extension of these methods and their computational codes to molecular targets is not straightforward, as several complications arise beyond the many-body nature of the problem, and not all of them can provide the correct asymptotic form. Different approaches have been applied to a large variety of molecules ranging from the smallest one, H₂, up to, e.g., DNA basis. The success of each method depends on the considered molecule and photon energy range, the validity of some approximations, and possibly on convergence issues or limitations related to the numerical implementation.

Except for small molecules, experimental data are not so abundant, and do not always span the whole photoelectron energy range; they therefore do not permit to fully assess the quality of different theoretical descriptions. As several theories are often not in agreement with each other and with experimental data, especially close to threshold, we made a survey of the different methods applied to PI in molecules. For each, we briefly indicate the main ingredients, the advantages and possible limitations. We also found useful to draw a list (rather complete to the best of our knowledge) of all molecules for which PI has been investigated theoretically.

136 In order to calculate the transition amplitudes for single PI in atomic or
 137 molecular systems, many considerations must be taken into account. Usually
 138 the starting point is the treatment of the ionized electron as a one-electron func-
 139 tion, the one-center expansion (OCE). In many cases, the vibrational structure
 140 of the molecule can be ignored, especially in high energy collisions, so that one
 141 may work within the Born–Oppenheimer (BO) approximation. Also, in order
 142 to simplify the calculations, the frozen core (FC) approximation and the static
 143 exchange approximation (SEA) are considered. It is within this frame, together
 144 with a model molecular potential, that we implement the generalized Sturmian
 145 approach. In the literature several Sturmian functions implementations exist,
 146 as reviewed, e.g., in the introductions of References 22 and 23. Similarly to pre-
 147 vious publications on scattering studies (see the recent review 22 and references
 148 therein), in this contribution we shall name *Generalized Sturmian Functions*
 149 (GSF) those defined in Section 5.1; note that other authors use the same termi-
 150 nology to define a different class of Sturmian functions. One of the advantages
 151 of such a method is that it allows to ensure that the continuum wavefunction
 152 has the correct asymptotic behavior²². To assess the validity of our approach,
 153 we will compare the calculated PI cross sections for a number of small molecules
 154 with theoretical and experimental data found in the literature.

155 The rest of this paper is organized as follows. We start with some gener-
 156 alities on PI in Section 2; we continue in Section 3 with a brief panorama of
 157 what sort of agreement one observes in the literature between theoretical and
 158 experimental cross sections. In Section 4 we present a survey of different theo-
 159 retical methods used to investigate molecular PI. In Section 5 we introduce the
 160 Sturmian approach, and compare our results for PI of H₂O, NH₃ and CH₄ to
 161 several theoretical and experimental data.

162 Atomic units ($\hbar = e = m_e = 1$) are assumed throughout, unless stated
 163 otherwise.

164 2 Generalities

165 In the study of the interaction of a radiation field (a photon) with a molecular
 166 target several processes may occur. Consider a photon of energy $E_\gamma = \hbar\omega$, such
 167 that $E_\gamma > I_0$, where I_0 is the ionization potential of the molecule. Once it
 168 strikes the polyatomic molecule RA in an initial vibrational state ν_0 (R is the
 169 polyatomic radical and A is an individual atom), the different outcomes may be

$$170 \quad \hbar\omega + \text{RA}(\nu_0) \rightarrow \begin{cases} \text{RA}^+ + e^-(\ell) & \text{Photoionization,} \\ \text{R}^* + \text{A}^* & \text{Photodissociation,} \\ \text{R}^* + \text{A}^{+*} + e^-(\ell) & \text{Dissociative photoionization.} \end{cases} \quad (1)$$

171 If we have a dissociation process, the final products can be in an excited state.
 172 If we have an ejected electron, called photoelectron, it has a defined angular
 173 momentum ℓ . In this contribution, we will concentrate only on single PI which
 174 can be considered as a “half-scattering” processes. It involves a bound-free
 175 transition for which one needs to know only the initial state Ψ_0 of the molecule,
 176 usually its ground state (energy E_0), and the final state of the ionized electron.
 177 The transition operator, that connects both initial and final states, is described
 178 semi-classically via the dipolar approximation; the dipolar operator in both

length (L) and velocity (V) gauges reads

$$\widehat{D}^{(L)} = -\hat{\mathbf{e}} \cdot \mathbf{r}, \quad (2a)$$

$$\widehat{D}^{(V)} = -\hat{\mathbf{e}} \cdot \mathbf{p}, \quad (2b)$$

where $\hat{\mathbf{e}}$ gives the polarization of the field. In this work we consider linear polarization along the z direction.

The major task is to calculate accurately the wavefunction Ψ of the photoelectron, that is an electron in a continuum state of the ionized molecular target, with an energy $E = k^2/2$ defined by the energy of the incident photon $E = E_\gamma - I_0$. Such continuum wavefunctions are more difficult to calculate than the low-lying bound-states as they oscillates up to infinity. They are solutions of the time-dependent Schrödinger equation (TDSE) or the time-independent Schrödinger equation (TISE), with well defined properties. They must be regular at the origin of the coordinate system, and the asymptotic boundary conditions are given by the superposition of an incoming-wave Coulomb function plus an incoming spherical wave, generated by the non-Coulomb part of the molecular potential²⁵

$$\lim_{r \rightarrow \infty} \Psi^{(-)} \propto e^{-i(kz + \frac{Z}{k} \ln k(r-z))} + f(\hat{k}, \hat{r}) \frac{1}{r} e^{-i(kr - \frac{Z}{k} \ln(2kr))}, \quad (3)$$

where $f(\hat{k}, \hat{r})$ is the transition amplitude and $Z = -1$ for an initial neutral target.

One quantity that is measurable experimentally is the PI cross section, defined theoretically as

$$\frac{d\sigma}{dE} = \frac{\pi e^2}{m^2 \hbar^2 c} \omega^{(g)} \left| \langle \Psi_0 | \widehat{D}^{(g)} | \Psi \rangle \right|^2, \quad (4)$$

where $\omega^{(L)} = E - E_0$ or $\omega^{(V)} = (E - E_0)^{-1}$ and c is the speed of light.

In most experiments it is difficult to determine the spatial orientation of the molecule in a given laboratory frame. Only a few advanced experimental techniques can perform a full angle-resolved spectroscopy, such as the one based on ultrashort pump-probe laser pulses^{26,27} and the full kinematic experiments as COLTRIMS (cold target recoil ion momentum spectroscopy)²⁸. In most cases, therefore, one must consider a random orientation of the molecule when it interacts with the radiation field. To do that, two different coordinates systems, whose origin coincide with the center of mass of the target, are considered²⁹: the laboratory frame, \mathbf{r}' , defined by the polarization axis of the electric field, and a molecular-fixed frame, \mathbf{r} , defined by the axis of highest symmetry. Let β and α be the polar angles of this molecular axis with respect to the laboratory frame, and let the set of Euler angles $\hat{\mathfrak{R}} = (\alpha, \beta, \gamma)$ denote hereafter the molecular orientation. A rotation $\hat{\mathfrak{R}}$ will bring the molecular fixed frame into coincidence with the laboratory frame. The dipolar operator in length gauge (2a), for a linearly polarized field (axis z), in the laboratory frame is then

$$z' = \left(\frac{4\pi}{3} \right)^{1/2} r \sum_{\mu} Y_1^{\mu}(\hat{r}) \mathcal{D}_{0\mu}^1(\hat{\mathfrak{R}}), \quad (5)$$

where $\mathcal{D}_{0\mu}^1(\hat{\mathfrak{R}})$ is the rotation matrix³⁰ that rotates the dipolar operator to the molecular frame. The rotated dipolar operator in velocity gauge follows

220 a similar expression. In order to calculate a cross section for a randomly ori-
 221 ented molecule, we must calculate first the orientation-dependent transition
 222 amplitudes in Equation (4) (see also Section 5.2) and then perform an angular
 223 average over $\hat{\mathfrak{R}}$, defined as

$$224 \quad \int d\hat{\mathfrak{R}} \equiv \frac{1}{8\pi^2} \int_0^{2\pi} d\alpha \int_0^\pi \sin\beta d\beta \int_0^{2\pi} d\gamma, \quad (6)$$

225 of the square modulus of such transition amplitudes.

226 3 Examples Taken from the Literature

227 As mentioned in the Introduction, many different theoretical methods and com-
 228 putational codes have been developed over the years to study PI in multielectron
 229 atoms. For molecules, many complications arise. The problem is highly non-
 230 central and generally multicenter so that continuum wavefunctions are quite
 231 difficult to calculate. Additionally the vibrational structure can have an impor-
 232 tant influence on the electronic structure and therefore on the PI itself.

233 To overcome all these complexities, additional to the “traditional” frozen
 234 core (FC) or the SEA, one starts to separate the electronic motion from that
 235 of the nuclei, and this is done using the BO approximation. One may also
 236 implement the fixed nuclei (FN) approximation, and it is possible to go further
 237 and use the OCE, where all electrons are referred to a common center, usually
 238 the center of mass of the molecule. Such variety of approximations (which
 239 are needed to deal with molecular systems), together with the choice of basis
 240 functions or adopted numerical approach, translates into a considerable non-
 241 uniformity in the quality of the end product. Except for H₂, for most molecules
 242 the PI cross sections obtained using different theoretical or numerical methods
 243 do not show an overall satisfactory agreement on one hand between them and,
 244 on the other hand, with experimental data. This is illustrated below with four
 245 different molecules: H₂, N₂, CO₂ and C₆H₆. We emphasize that almost all
 246 experimental data presented here do not have explicit error bars, either because
 247 they are not indicated in the given references or because they are too small,
 248 typically smaller than 3%.

249 3.1 H₂

250 We start with H₂, the simplest many-electron molecule. Figure 3.1 shows the
 251 PI cross sections obtained using different methods: self-consistent field (SCF,
 252 see Section 4.2.1), configuration interaction (CI, see Section 4.1), ground state
 253 inversion method (GIPM/D, see Section 4.7.2), random-phase approximation
 254 (RPA, see Section 4.9) and logarithmic derivative Kohn method (LDKM, see
 255 Section 4.11.1). They are further compared with the experimental data of Chung
 256 *et al*³¹. For this example, SCF and CI calculations used OCE, CBF used FN
 257 and LDKM the FC approximation. Except for the SCF results, we see an
 258 excellent agreement between all theories with experimental data. Indeed, the
 259 molecule H₂ is sufficiently simple to allow for a PI study taking into account
 260 all interactions. One aspect, though, that remains challenging is to calculate
 261 precisely the positions and widths of the doubly excited states that depend on
 262 the nuclear motion.

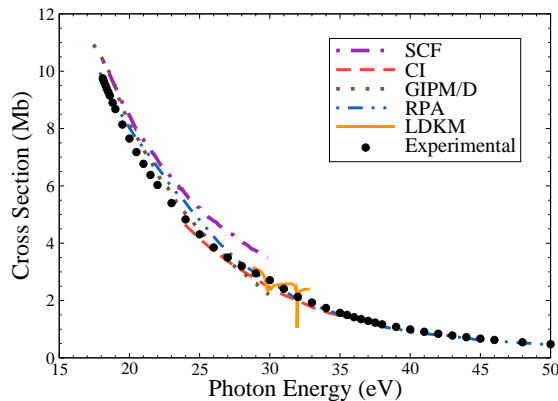


Figure 3.1: (Color online) PI cross section in Mb versus photon energy in eV for the ground state of H_2 molecule. We compare the results obtained using SCF³² (purple, dash-dot); CI³³ (red, dash); GIPM/D³⁴ (brown, dots); RPA³⁵ (blue, dash-dot-dot) and LDKM³⁶ (orange, solid) with experimental data³¹ (black dots).

263 3.2 N_2

264 We show in Figure 3.2 the PI cross sections for the outer valence orbital $3\sigma_g$ of
 265 N_2 . For such MO we show calculations performed with CI (Section 4.1), time-
 266 dependent density functional theory (TD-DFT, see Section 4.3.2), multiple-
 267 scattering $X\alpha$ (MS $X\alpha$, see Section 4.6), Stieltjes–Tchebycheff technique (STT,
 268 see Section 4.10) and iterative–Schwinger method (ISM, see Section 4.12.1).
 269 Note that the results for CI and TD-DFT were obtained using OCE, and for
 270 ISM using the FC approximation. The theoretical cross sections are compared
 271 with the experimental results of Plummer *et al*³⁷.

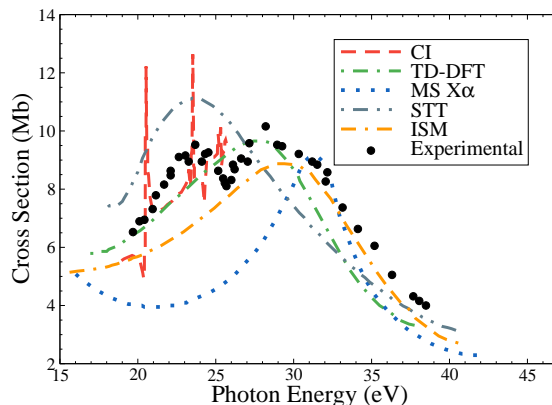


Figure 3.2: (Color online) Partial PI cross section in Mb versus photon energy in eV from the MO $3\sigma_g$ of N_2 . Results for CI³⁸ (red, dash); TD-DFT³⁹ (green, dash-dot); MS $X\alpha$ ⁴⁰ (blue, dots); STT⁴¹ (gray, dash-dot-dot) and ISM⁴² (orange, dash-dash-dot) are compared with experimental data³⁷ (black dots).

272 The situation changes drastically when moving from H_2 to a more complex

273 molecule such as N_2 . The Figures show that the agreement between different
 274 theories and experimental data is basically lost, especially for energies close to
 275 threshold. Moreover, only a partial agreement for higher energies is observed.
 276 Except for the CI results, none of the other calculations reproduces the different
 277 series of resonances located between 20 and 25 eV.

278 3.3 CO_2

279 The PI cross sections for CO_2 are shown in Figure 3.3 for the MO $1\pi_g$. We
 280 compare the results obtained with GIPM/D (Section 4.7.2), STT (Section 4.10),
 281 ISM (Section 4.12.1) and R -matrix method (RMM, see Section 4.8). The ex-
 282 perimental data are taken from Brion and Tan⁴³.

283 Here, results for ISM and RMM used both the FC and the FN approxi-
 284 mations. Depending on the energy range, the different theoretical calculations
 285 present again only a partial agreement, and even if they cannot reproduce com-
 286 pletely the experimental data, they perform rather well beyond 25 eV. Although
 287 the center of mass of CO_2 is close to the C atom because of its linear geom-
 288 etry, this molecule is particularly difficult to describe: the density of charge
 289 is completely delocalized around the molecule and only the use of multicenter
 290 wavefunctions yields acceptable PI results, as in the GIPM/D case.

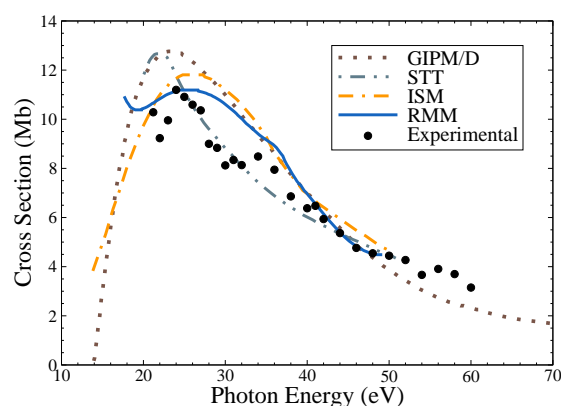


Figure 3.3: (Color online) Partial PI cross section in Mb versus photon energy in eV from the MO $1\pi_g$ of CO_2 . Results for GIPM/D⁴⁴ (brown, dots); STT⁴¹ (gray, dash-dot-dot); ISM⁴⁵ (orange, dash-dash-dot) and RMM⁴⁶ (blue, solid) are compared with experimental data⁴³ (black dots).

291 3.4 C_6H_6

292 Finally, for benzene (C_6H_6), PI cross sections for the outer valence orbital $1e_{1g}$
 293 are shown in Figure 3.4. The theoretical results obtained using DFT (Sec-
 294 tion 4.3.1), TD-DFT (Section 4.3.2), GIPM/D (Section 4.7.2) and LDKM (Sec-
 295 tion 4.11.1) are compared with the experimental data by Carlson *et al*⁴⁷.

296 This is a rather complex molecule to describe theoretically, and the difficul-
 297 ties show up in the PI spectra. None of the calculations reproduce accurately
 298 the resonances (neither their energy position nor their intensity), let alone the
 299 overall cross section magnitude except at rather high photoelectron energies.

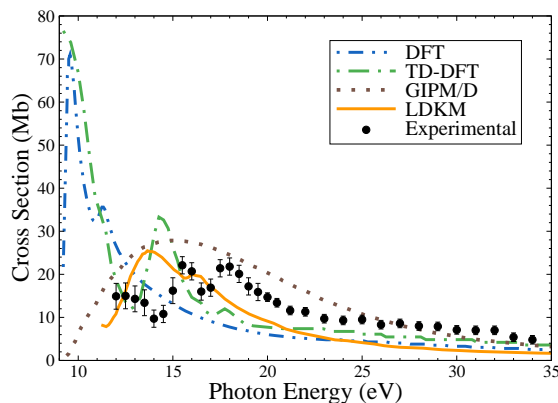


Figure 3.4: (Color online) Partial PI cross section in Mb versus photon energy in eV from the MO $1e_{1g}$ of C_6H_6 (benzene). Results for DFT⁴⁸ (blue, dash-dot-dot); TD-DFT⁴⁹ (green, dash-dot); GIPM/D⁵⁰ (brown, dots) and LDKM⁵¹ (orange, solid) are compared with experimental data⁴⁷ (black dots).

300 As evidenced from Figures 3.1 to 3.4, except for H_2 , for all other molecules
 301 we can draw similar conclusions: (1) large disagreements between methods are
 302 clearly observable when comparing PI cross sections; (2) experimental data, in
 303 particular near threshold, are generally not well reproduced (other features of
 304 the continuum spectra are also difficult to reproduce). This is also true for H_2O ,
 305 NH_3 or CH_4 molecules; the cross sections will be presented in Section 5.3, where
 306 we shall compare different theoretical calculations including ours obtained with
 307 the Sturmian approach. To have an overview of most methods that have been
 308 proposed to describe molecular PI, we present in the next section a survey and
 309 indicate to which molecules they have been applied (a rather complete list is
 310 presented in Appendix A).

311 4 Survey of Theoretical Methods

312 4.1 CI

313 One of the “classical” methods used to study electronic structure in atoms and
 314 molecules is configuration-interaction (CI); a description of its use for the study
 315 of PI of molecules can be found in Reference 52.

316 Some results obtained using the CI method are the studies by Daasch *et al*⁵³
 317 for CO_2 , van Dishoeck *et al*⁵⁴ for HCl and Decleva *et al*⁵⁵ for O_3 . Using B-
 318 splines⁵⁶ as a basis set, Apalategui and Saenz⁵⁷ studied multiphoton ionization
 319 of H_2 ; Vanne and Saenz⁵⁸ studied HeH^+ ; Fojón *et al*⁵⁹ also studied H_2 ; Sanz-
 320 Vicario *et al*³³ studied PI of H_2 by ultrashort laser pulses and Sansone *et al*²⁷ for
 321 H_2 and D_2 ; Doweck *et al*⁶⁰ studied circular dichroism in H_2 . Using the so-called
 322 time-dependent CI⁶¹, we find the works of Klinkusch *et al*⁶² for LiCN, and of
 323 Sonk and Schlegel⁶³ for C_4H_6 (butadiene). Finally, using the multichannel CI
 324 complete-active-space⁶⁴, we can find the works of Stratmann *et al*³⁸ for N_2 , and
 325 of Stratmann and Lucchese⁶⁵ for O_2 .

4.2 Hartree–Fock Methods

4.2.1 Self-Consistent Field

Among the studies that have used the Hartree–Fock (HF) method and the self-consistent field (SCF) to study PI of molecules, we find the work of Dalgarno⁶⁶ for CH₄; Kelly³² studied H₂; Schirmer *et al*⁶⁷, together with the Green’s function formalism, studied the inner-valence PI of N₂ and CO; Padial *et al*¹, using Gaussian-type orbitals (GTOs), studied C₂. For calculations performed with the relaxed-core HF approximation, we have the results of Larkins and Richards⁶⁸ for Li₂; the studies of Saito *et al* on the *K*-shell photoelectron angular distribution from CO₂⁶⁹ and from NO₂⁷⁰; Semenov *et al*⁷¹ studied the PI from the *K*-shell of the CO. We should also mention the review of different applications of SCF by Ågren *et al*⁷².

4.2.2 Multiconfiguration time-dependent Hartree–Fock

In general, it is difficult to describe with high precision highly excited states and non-adiabatic dynamics in molecules, especially if one is interested in studying ionization by high-intensity radiation fields. The multiconfiguration time-dependent Hartree–Fock (MCTDHF) approach is a method that uses a linear combination of determinants of time-dependent orbitals, and is flexible enough to describe the response of a molecule to short and intense laser pulses. The formalism can be found in References 73–75.

The MCTDHF has been used by Kato and Kono⁷⁵ and by Haxton *et al*⁷⁶ to study PI of H₂ by intense laser fields, and also by Haxton *et al*⁷⁷ for HF.

4.3 Density Functional Theory

The density functional theory (DFT) is widely used in quantum chemistry. It allows to determine easily the electronic structure of a given system (an atom, a molecule, a crystal, etc), regardless of its extension or the number of particles that constitute it. While “standard” quantum mechanics works directly with the many-body wavefunctions of the different particles in a given system, the DFT uses the one-electron electronic density $n(\mathbf{r})$, and is based on two theorems, called the Hohenberg–Kohn theorems⁷⁸. In different implementations of the DFT to study PI of molecules, $n(\mathbf{r})$ is calculated using a conventional linear combination of AOs (LCAO)⁴⁸.

4.3.1 Kohn–Sham DFT

In the Kohn–Sham DFT (KS DFT)⁷⁹, the Hamiltonian of the molecular system is determined by the density of the occupied orbitals in the ground state, and in terms of the Hartree potential, the electron-nuclei interaction, and the so-called exchange-correlation potential which contains all the “unknowns” of the system. Different potentials are available in the literature for different atomic and molecular systems (see, for instance References 80 and 81), based, for example, in the local density approximation or in the generalized gradient approximation.

The KS DFT has been used by Venuti *et al*⁴⁸ to study PI in C₆H₆; by Stener and Decleva, using the OCE approximation, to study HF, HCl, H₂O, H₂S, NH₃ and PH₃ (Reference 82), and CH₄, SiH₄, BH₃ and AlH₃ (Reference

369 83). Toffoli *et al*⁸⁴, using the multicenter expansion, calculated cross sections
 370 for Cl₂, (CO)₂ and Cr(CO)₆. Woon and Park⁸⁵ also studied C₆H₆ (benzene),
 371 C₁₀H₈ (naphthalene), C₁₄H₁₀ (anthracene) and C₁₆H₁₀ (pyrene). Stranges *et*
 372 *al*⁸⁶ studied the dynamics in circular dichroism of the C₃H₆O (methyl-oxirane).
 373 Toffoli *et al*⁸⁷ studied the PI dynamics in C₄H₄N₂O₂ (uracil).

374 4.3.2 Time-Dependent DFT

375 The time-dependent DFT (TD-DFT)⁸⁸ constitutes another line of development
 376 of the DFT methods. In the first order time-dependent perturbative scheme,
 377 where the zeroth order is equivalent to the KS DFT⁸⁹, the linear response of
 378 the electronic density $n(\mathbf{r})$ to an external weak time-dependent electromagnetic
 379 field can be described by a SCF potential, given by Zangwill and Soven⁹⁰.

380 The TD-DFT has been used by Levine and Soven³⁹ to calculate photoe-
 381 mission cross sections and asymmetry parameters of N₂ and C₂H₂. Stener,
 382 Decleva and coworkers, using B-splines⁵⁶ and the OCE, studied PI for different
 383 molecules: Stener and Decleva⁸⁹ calculated the cross sections for N₂ and PH₃;
 384 Stener *et al*⁹¹ for CH₄, NH₃, H₂O and HF; Stener *et al*⁹² for CO and also from
 385 the *K*-shell⁹³; Fronzoni *et al*⁹⁴ for C₂H₂; Stener *et al*⁴⁹ for CS₂ and C₆H₆;
 386 Toffoli *et al*⁹⁵ and Patanen *et al*⁹⁶ for CF₄, and Holland *et al*⁹⁷ for pyrimidine
 387 and pyrazine. We also find the work of Russakoff *et al*⁹⁸ for C₂H₂ and C₂H₄,
 388 and by Madjet *et al*⁹⁹ for C₆₀. Different results for molecular PI have been
 389 reviewed by Stener *et al*¹⁰⁰.

390 For the sake of completeness, we also mention some studies of molecular PI
 391 that use a slightly different approach, the static-exchange DFT: Plésiat *et al*¹⁰¹
 392 investigated PI of N₂ and CO, and Kukk *et al*¹⁰² from the inner-shells of CO.

393 4.4 Complex Methods

394 4.4.1 Complex Scaling

395 The complex scaling (CS) method^{103,104} has been used extensively to study
 396 ionization and, mainly, resonance phenomena in atoms and molecules. The idea
 397 behind this method is to scale the coordinates of all particles in the Hamiltonian
 398 by a complex-valued scale factor: $r \rightarrow re^{i\theta}$. One variant of the CS is the so-
 399 called exterior complex scaling (ECS)¹⁰⁵⁻¹⁰⁷, whereby the coordinates scale only
 400 outside a fixed radius R_0

$$401 \quad r \rightarrow R(r) = \begin{cases} r & \text{for } r \leq R_0, \\ R_0 + (r - R_0)e^{i\theta} & \text{for } r > R_0. \end{cases} \quad (7)$$

402 The ECS method has been applied to study general scattering problems using L^2
 403 basis set representations. It is especially well suited to study ionization processes
 404 in molecules, since the definition of the exterior scaling (7) avoids complicated
 405 scaling expressions in the nuclear attraction terms of the Hamiltonian¹⁰⁶ when
 406 R_0 is large enough to enclose all the molecular nuclei.

407 The ECS has been used mainly by McCurdy, Rescigno, Martín and coworkers
 408 to study different ionization processes in atoms and molecules: McCurdy and
 409 Rescigno^{108,109} used Cartesian Gaussian-type orbitals (CGTOs) to calculate PI
 410 cross sections of H₂⁺; Vanroose *et al*^{110,111}, using B-splines⁵⁶, studied double
 411 PI (DPI) of H₂; Rescigno *et al*¹¹² performed *ab initio* DPI calculations of H₂;

412 Tao *et al*, using discrete variable representation (DVR)¹¹³, calculated PI cross
413 sections for H_2^+ ^{114,115} and angular distribution for DPI of H_2 ¹¹⁶.

414 4.4.2 Complex Basis Functions

415 In the complex basis functions (CBF) technique^{108,109,117} (the CS method can
416 be considered a particular case of the CBF where the basis functions are defined
417 in terms of the physics of the problem) the continuum scattering information is
418 extracted from a finite-matrix representation of the electronic Hamiltonian in a
419 set of complex square-integrable basis functions. The resulting matrix elements
420 necessary to obtain the cross section, can be calculated efficiently using a discrete
421 basis set approximation to the spectrum of the Hamiltonian¹⁰⁸.

422 The CBF technique, together with complex GTO, has been used by Mc-
423 Curdy and Rescigno¹⁰⁸ to calculate PI cross section of H_2^+ ; by Yu *et al*¹¹⁷ for
424 valence- and *K*-shell ionization of N_2 , and by Morita and Yabushita¹¹⁸ for H_2^+
425 and H_2 .

426 4.5 Linear Algebraic Method

427 The linear algebraic method (LAM), developed by Collins and Schneider^{119,120},
428 has been applied successfully to study molecular excitation and ionization by
429 electron collisions. The adaptation of the method to study PI in molecules is
430 given explicitly in Reference 121. The LAM presents the advantage of including
431 explicitly an effective optical potential in order to introduce correlation effects
432 into the scattering solution¹²¹.

433 While the initial state is treated separately, usually in terms of GTO or
434 CGTO¹¹⁹, the method is used to calculate directly the ejected electron un-
435 bound wavefunction that satisfies the TISE. To do so, the configuration space
436 is divided into two regions, with the boundary at $r = a$: (1) for $r \geq a$, where
437 nonlocal effects are negligible, the wavefunction can be calculated by standard
438 propagation procedures; (2) for $r < a$, where exchange and correlation effects
439 are important, the wavefunction is expanded in two terms: one as a linear com-
440 bination of the wavefunctions of the molecular-ion target and the scattering
441 wavefunction, and the other in a set of “correlation” functions that are added
442 for completeness¹²¹.

443 In the LAM one obtains a set of differential equations in the SEA, that can be
444 converted into a set of radial integro-differential equations using an expansion
445 in partial waves of the electronic wavefunctions. Then, this set of scattering
446 equations is further transformed into a set of coupled integral equations using
447 Coulomb Green’s functions¹¹⁹. Finally, by introducing a discrete quadrature to
448 evaluate the integrals, one obtains a set of linear-algebraic equations that can
449 be solved with standard linear systems routines. This solution must be matched
450 at $r = a$ with the result of the propagation scheme to the asymptotic region.
451 More details on the effective optical potential are given in the References 121,
452 119 and 122.

453 To our knowledge, this method has been used only by Collins and Schnei-
454 der¹²¹ to calculate cross sections for H_2 , N_2 , NO and CO_2 .

4.6 Multi-Scattering

The multiple-scattering method (MSM) has been developed in different physics fields, as in nuclear physics¹²³, solid state physics¹²⁴, and also in atomic and molecular physics (see, for example, References 125 and 126, and references therein). The idea behind the MSM is to represent the molecular field, that in general is highly non-central in the molecular core region, by a set of three potentials V_I , V_{II} and V_{III} , defined in different non-overlapping spheres (called muffin-tin partitioning): (I) defined by the $\{I_i\}$ spherical regions containing the different atomic nuclei at their center $r_i = 0$, and with radii $\{\rho_i\}$; (II) defined by $r_i > \rho_i$ and $r_0 < \rho_{III}$, where r_0 is the radial coordinate from the center of the molecule and ρ_{III} is the outer sphere radius, measured from the molecular center. In general, the potential V_{II} is considered constant; (III) defined by $r_0 \geq \rho_{III}$. The potential V_{III} has a spherical symmetry. One can construct the photoelectron continuum wavefunction taking into account the continuity conditions between all three regions, and imposing the incoming boundary conditions (3) in the external region. The total wavefunction is written as $\Psi = \sum_i \Psi_i + \Psi_{II} + \Psi_{III}$, where each term is a solution to the potential of the corresponding region of the molecular field, and obeys the adequate asymptotic boundary conditions.

The MSM or, equivalently the multiple-scattering with an undetermined factor α (MS X α)¹²⁷, have been widely used to study ionization of molecules by photon and electron impact. For example, Davenport calculated cross sections for N₂ and CO^{40,128}, and for H₂¹²⁸; Dehmer and Dill calculated the *K*-shell PI of N₂¹²⁹; Grimm¹³⁰ calculated the cross section for C₂H₄ and Grimm *et al*¹³¹ for N₂, CO, CO₂, COS and CS₂; Rosi *et al*¹³² studied PI in CH₄ and CF₄; Tse *et al*¹³³ investigated the photoabsorption spectra in SiCl₄; Ishikawa *et al*¹³⁴ studied, implementing a DVR¹¹³ method, SiH₄, SiF₄ and SiCl₄; Powis studied PI in PF₃¹³⁵, CH₃I¹³⁶ and CF₃Cl¹³⁷. Finally, Jürgensen and Cavell¹³⁸ compared directly experimental results with the MS X α for NF₃ and PF₃.

4.7 Plane-Wave-Based Methods

4.7.1 Plane-Wave and Orthogonalized Plane-Wave Approximations

The simplest description of an ionized electron is the plane-wave approximation (PWA), but it is not expected to give accurate results near threshold¹³⁹. To our knowledge, the first implementations of the PWA are due to Kaplan and Markin^{140,141}, Lohr and Robin¹⁴², and to Thiel and Schweig^{143,144}.

The final state of the molecule describes one electron that has been excited from a given initial MO to a continuum normalized plane-wave orbital¹³⁹. This plane-wave is not necessarily orthogonal to any of the occupied MOs; if orthonormality is imposed, we have the orthogonalized PWA.

The PWA and the orthogonalized PWA, together with Slater-type orbitals (STOs) to describe AO, have been used by Rabalais *et al*¹⁴⁵ and by Dewar *et al*¹⁴⁶ to calculate PI cross sections for H₂, CH₄, N₂, CO, H₂O, H₂S and H₂CCH₂. Huang *et al*¹⁴⁷ used the orthogonalized PWA to calculate angular asymmetry parameters for H₂, N₂ and CH₄. Beerlage and Feil¹⁴⁸ calculated cross sections for HF, (CN)₂, CaHCN, C₂(CN)₂, N₂, CO, H₂O, furan, pyrole and tetrafluoro-pyrimidine. Schweig and Thiel¹⁴⁹ calculated the relative band intensity of N₂, CO, H₂O, H₂S, NH₃, PH₃, CH₄, (CH₃)₂S, C₆F₆, among others.

501 Hilton *et al*¹⁵⁰ have used the so-called effective PWA to calculate cross sections
502 for H₂, CO, H₂O and C₂H₄. Finally, Deleuze *et al*¹⁵¹ used the orthogonalized
503 PWA, together with a many-body Green's function framework, to calculate PI
504 cross sections for CH₄, H₂O, C₂H₂, N₂, and CO.

505 4.7.2 Ground Inversion Potential Method

506 The so-called ground state inversion potential method (GIPM) has been devel-
507 oped by Hilton, Hush, Nordholm and coworkers^{150,152} with the aim of obtaining
508 a chemical theory of PI intensities¹⁵³. This method uses the standard one-
509 electron PWA, the orthogonalized PWA or the energy shifted PWA¹⁵⁰ in order
510 to calculate the electronic continuum final wavefunction. The cross section is
511 obtained from an atomic summation theory together with a plane wave analysis
512 of diffraction effects from photoelectron amplitudes from different atoms that
513 interfere with each other^{34,153}. The main difference of GIPM with a standard
514 PWA is that the potential felt by an electron when leaving an atomic center in a
515 molecule is calculated directly by inversion of the ground state HF orbital^{152,153}.
516 The GIPM theory can include three important effects: the change in the nature
517 of the atomic orbitals upon formation of the molecule, diffraction effects¹⁵³ and
518 exchange in an exact way.

519 The GIPM has been used by Hilton *et al* to calculate PI cross sections for
520 H₂O¹⁵⁴ and for H₂, N₂ and CO³⁴. Also Kilcoyne *et al* calculated cross sections
521 for H₂, HF and N₂¹⁵³; H₂O, NH₃ and CH₄¹⁵⁵; CO, CO₂ and N₂O⁴⁴, and for
522 C₂H₄ and C₆H₆⁵⁰.

523 4.8 R-Matrix Method

524 Originally introduced in nuclear physics, the *R*-matrix method (RMM) has been
525 adapted to atomic and molecular physics by Burke and coworkers (see Reference
526 156 and references therein). Applications of this method, in particular for elec-
527 tron collisions, have been reviewed elsewhere¹⁵⁷⁻¹⁵⁹. The idea behind the RMM
528 is to enclose the scattering particles and the target within a sphere of radius *a*,
529 so that it should be possible to characterize the system using the eigenenergies
530 and the eigenstates computed within the sphere. Then by matching them to the
531 known asymptotic solutions, one can extract all the scattering parameters. The
532 *R*-matrix is defined as the matrix that connects the two regions in which the
533 space is divided into. They are: (1) an internal region, where all the particles
534 are close to one another, so that the short-range interactions and exchange are
535 important; (2) an external region, where all particles are still interacting, but
536 the forces are direct and could have a multi-polar character. In the most conven-
537 tional use of the RMM, the Hamiltonian of the internal region is diagonalized in
538 order to obtain the *R*-matrix eigenenergies and eigenfunctions, generally using
539 the non-adiabatic formalism¹⁶⁰. The initial and final states are expanded in
540 terms of these eigenstates. The corresponding coefficients for the initial state
541 are usually obtained by performing an all-channels-closed scattering calculation,
542 and in this case the problem is reduced to find the zeros of a determinant^{161,162}.
543 To obtain the coefficients for the final state, calculations of electron scattering
544 by the corresponding molecule can be performed, and the resulting *R* matrices
545 represent the result of a full non-adiabatic treatment of the internal region of
546 the scattering problem¹⁵⁹, and provides the solution in the external region¹⁶³.

547 Finally, with both sets of coefficients, it is possible to calculate the required
548 transition dipole moments, and thus the PI cross section (4).

549 Since the corresponding formalism is relatively new, the RMM has not been
550 used for molecules as much as for atoms. However, we have the works by
551 Tennyson *et al*¹⁶⁴ for H₂, and by Tennyson¹⁶⁵ for H₂ and D₂. The so-called *R*-
552 matrix Floquet theory^{166,167} has been used by Burke *et al*¹⁶⁷ and by Colgan *et*
553 *al*¹⁶⁸ to study multiphoton processes in H₂. Saenz¹⁶⁹, using STOs, studied PI
554 in HeH⁺. Tashiro¹⁷⁰ calculated cross sections for N₂ and NO. Finally, Harvey
555 *et al*⁴⁶ recently studied CO₂, using GTOs combined with Coulomb and Bessel
556 functions.

557 4.9 Random Phase Approximation

558 The random phase approximation (RPA) is a method that has been applied
559 with success to study PI in atoms and molecules^{171,172}. One advantage is that
560 PI cross sections calculated in length or velocity gauges coincide. Additionally,
561 the computational effort required in the RPA implementation is comparable to
562 calculations in the single active electron (SAE) approximation, since the RPA
563 uses only two-electron integrals involving two occupied and two unoccupied
564 orbitals^{173,174}.

565 In the standard procedure of the RPA, the ground state and the one-electron
566 wavefunctions for the excited and continuum states of the molecule are calcu-
567 lated at HF level. With these, all required matrix elements and in particular
568 the Coulomb and dipole matrix elements, can be calculated directly. Next, the
569 RPA dipole matrix elements are calculated solving the corresponding equation,
570 and the results are used to obtain directly PI cross sections or the required
571 observables^{173–176}.

572 The RPA has been used to study PI of H₂ by Martin *et al*³⁵, by Schirmer
573 and Mertins¹⁷⁷ and by Semenov and Cherepkov^{176,178}. For N₂ we can find
574 calculations performed by Lucchese and Zurales¹⁷⁹; by Semenov and Cherep-
575 kov^{175,180}; by Yabushita *et al*¹⁷⁴, using complex functions; and by Montuoro
576 and Moccia¹⁸¹, using mixed L^2 basis sets (STOs and B-splines⁵⁶). For H₂S
577 we have the results of Cacelli *et al*¹⁸². For LiH, calculations were performed
578 by Carmona–Novillo *et al*¹⁸³. For C₂H₂ we have the results of Yasuike and
579 Yabushita¹⁸⁴, who used complex basis functions (see Section 4.4.2), and by
580 Montuoro and Moccia, using the mixed L^2 basis sets. We can find also calcula-
581 tions for the *K* shell of N₂ by Cherepkov *et al*¹⁸⁵; for the ion C₆₀⁺ by Polozkov
582 *et al*¹⁸⁶, or for the fullerenes C₂₀ and C₆₀ by Ivanov *et al*¹⁸⁷. Extensive calcu-
583 lations have been performed by Cacelli *et al*¹⁸⁸, to study PI in CH₄, NH₃, H₂O
584 and HF, and by Amusia *et al*¹⁷¹, who used the RPA with exchange to calculate
585 PI cross sections of CH₄, C₂H₆, C₃H₈, C₂H₄, C₂H₂, NH₃, H₂O, CN⁻, N₂, CO,
586 CO₂, N₂O and NO₂.

587 4.10 Stieltjes–Tchebycheff Technique

588 The Stieltjes–Tchebycheff technique (STT), developed by Langhoff and cowork-
589 ers (see, for example, References 189 and 190 and references therein), is based
590 on theorems from the theory of moments¹⁹¹; its flexibility allows the use of
591 different type of basis sets^{190,192,193}. The technique has been widely and suc-
592 cessfully used to study ionization processes in different atomic and molecular

593 systems.

594 The strength of the interaction of unpolarized radiation with a target gas can
 595 be described by Kramers–Heisenberg expression of the polarizability (frequency-
 596 dependent) of the constituent molecules. This strength can be written as a
 597 Stieltjes integral over the appropriate oscillator strength distribution^{189,193} or,
 598 alternatively, by the use of the cumulative oscillator-strength distribution which
 599 can be approximated by an histogram (Stieltjes procedure). Even if such an his-
 600 togram cannot represent adequately the continuum of the molecule, it can give
 601 good approximations to the related power moments, and it rigorously bounds
 602 the correct distribution through Tchebycheff inequalities¹⁹¹. More technical de-
 603 tails about the direct computational implementation of the STT are provided
 604 in Reference 190.

605 The STT has been used to study PI in CH, using STOs, by Barsuhn and
 606 Nesbet¹⁹⁴; in H₂, using GTOs in a CI method (see Section 4.1), by ONeil
 607 and Reinhardt¹⁹⁵; in N₂, together with GTOs, by Rescigno *et al*¹⁹³ and using
 608 LCAO with optimized STOs by Stener *et al*⁴¹. In H₂O by Williams *et al*¹⁹⁶
 609 and by Delaney *et al*¹⁹⁷ in the SEA, both using GTOs; by Diercksen *et al*¹⁹⁸,
 610 using Cartesian Gaussian basis sets and by Cacelli *et al*¹⁹⁹ using STOs in the
 611 independent-channel approximations. By Cacelli *et al*, we also find calculations
 612 for NH₃¹⁹⁹, HF²⁰⁰, HCl²⁰¹, H₂S²⁰² and CH₄²⁰⁰. For CO we mention the work
 613 by Göring and Rösch²⁰³, who used GTOs. For F₂, Orel *et al*²⁰⁴ used contracted
 614 Gaussians. For C₆H₆ Gokhberg *et al*²⁰⁵ used the STT together with the Lanczos
 615 algorithm. Finally, Stener *et al*⁴¹ have performed calculations using LCAO with
 616 optimized STOs for CO₂, N₂O, SF₆, C₂N₂, TiCl₄ and Cr(CO)₆.

617 4.11 The Kohn Variational Method

618 Among different approximate methods used to determine the energy spectra
 619 and the corresponding wavefunctions, we have the perturbation theory and the
 620 standard Ritz variational method²⁵, where approximate solutions of the TDSE
 621 or the TISE for a given problem are found in a subspace of the real prob-
 622 lem. Besides the standard Ritz method, there is also, e.g., the Kohn variational
 623 method (KVM)²⁰⁶. The idea behind the latter is to find a variational expres-
 624 sion that allows one to calculate the wavefunction with a correct asymptotic
 625 behavior. This is dictated by two arbitrary $f_\ell(r)$ and $g_\ell(r)$ functions, that be-
 626 have asymptotically as the regular $F_\ell(kr)$ and, respectively, irregular $G_\ell(kr)$
 627 Coulomb functions. The trial wavefunction can be written as

$$628 \quad \psi_\ell^t(r) = f_\ell(r) + \lambda^t g_\ell(r) + \sum_i c_i \varphi_i(r), \quad (8)$$

629 where $\{\varphi_i\}$ is a set of L^2 functions and λ^t is a trial parameter. The Kato iden-
 630 tity²⁰⁷ is used to find a stationary λ^s value. We can distinguish two options for
 631 the trial wavefunction (8): (1) if f_ℓ and g_ℓ are the regular and irregular Coulomb
 632 functions, then we have $\lambda = \tan \delta_\ell$, where δ_ℓ is the phase shift related to a short
 633 range potential; (2) if g_ℓ is an outgoing function $h_\ell^{(-)}$, called “regularized” ir-
 634 regular Coulomb function (defined as $h_\ell^{(-)}(r) = ik^{-1/2} [F_\ell(kr) - ic(r)G_\ell(kr)]$,
 635 where $c(r)$ is a cutoff function) then $\lambda = e^{i\delta_\ell} \sin \delta_\ell$, i.e., the T -matrix (transition
 636 matrix). In this case we have the complex Kohn method^{207,208}.

637 Two different implementations of the KVM in the study of PI of molecules
 638 are separately hereafter described.

639 4.11.1 Logarithmic Derivative Kohn Method

640 The logarithmic derivative Kohn method (LDKM)^{209,210}, and its variant, the
 641 finite-volume variational method²¹¹, were originally proposed to generate a
 642 translational basis for reactive scattering, using Lobatto shape functions^{210,212,213}.
 643 In this method, all the required radial integrals are performed explicitly over a
 644 finite volume V , usually a sphere. The main difference between the LDKM and
 645 the standard KVM is that different coefficients are added to the functions f_ℓ
 646 and g_ℓ in (8); these coefficients can be determined by matching the wavefunc-
 647 tion and their derivatives with the exact Coulomb functions across the surface
 648 that delimits the integration volume V ^{51,213}. In many of the implementations
 649 of the LDKM, Lobatto shape functions, referred usually as free-type functions,
 650 are used as the basis set $\{\varphi_i\}$ in (8).

651 The LDKM has been used to calculate PI cross sections for H_2^+ by Le Rouzo
 652 and Raşeev²¹¹, and by Rösch and Wilhelmy²¹³; Raşeev³⁶ studied autoioniza-
 653 tion in H_2 ; and Wilhelmy *et al*^{51,214} calculated cross sections and asymmetry
 654 parameters for N_2 , CO and C_6H_6 .

655 4.11.2 Complex Kohn method

656 The complex Kohn method (CKM), developed by McCurdy, Rescigno and
 657 coworkers to study excitation and ionization of molecules by electron colli-
 658 sions^{208,215,216}, have proved to be very effective, in particular in the first-order
 659 calculation of dipolar transition moments²¹⁵. The adaptation of the method to
 660 study PI in molecules has been described by Lynch and Schneider²¹⁷. Different
 661 elections of the arbitrary cutoff function $c(r)$ or the irregular function $g_\ell(r)$
 662 have been tested^{217,218}.

663 The CKM has been used Lynch and Schneider²¹⁷ to study PI of H_2 and
 664 N_2 ; by Rescigno *et al*²¹⁹ to study CO , examining the effects of the interchannel
 665 coupling; Orel and Rescigno²²⁰ to study NH_3 and, more recently, Jose *et al*²²¹
 666 to study PI of SF_6 also adding interchannel coupling effects.

667 4.12 The Schwinger Variational Method

668 While many variational methods are based on the TISE (a differential equation),
 669 several others, as the Schwinger variational method (SVM)²²² are based on the
 670 equivalent integral equation, the Lippmann–Schwinger equation (LSE)^{223,224}.

671 The advantage of the LSE over the TISE to study collisions processes is that
 672 the correct boundary conditions of the problem are automatically incorporated
 673 through the use of the corresponding Green function G^C . The SVM is a powerful
 674 formulation of the scattering problem that can provide highly accurate solutions
 675 without requiring expansions in very large basis sets^{225,226}. The idea behind
 676 this method is to obtain a stationary variational condition over the T -matrix.
 677 In general, one can obtain better converged results using the SVM compared to
 678 the KVM results.

679 The implementation of the SVM has been developed along two methods,
 680 named the Schwinger multichannel method²²⁷ and the iterative-Schwinger method
 681 (ISM). The latter, and a variant using continued fractions, are now briefly de-
 682 scribed.

4.12.1 Iterative Schwinger

The ISM is an iterative approach to the solution of collisions problems using the SVM²²⁵ to solve the LSE. The first implementation of ISM^{226,228,229} was the study of scattering of low-energy electrons by atoms and molecules. In the case of molecules, the fixed-nuclei approximation was used together with the assumption that the interaction between the ionized electron and the molecular ion is described by the static-exchange potential^{229,230}. The description of the ISM implementation to study PI is given with details in References 42 and 45.

In the ISM instead of solving the associated LSE for each partial-wave of the scattering function, one solves equivalently a LSE for the T matrix^{225,230}: $T = U + UG^CT$. The iterative method begins by approximating the short-range potential U by a separable potential \tilde{U} , using an initial set of expansion functions R ; then the scattering solutions for the approximate potential \tilde{U} are obtained from the corresponding LSE. The iterative procedure is continued by augmenting the original set of functions with those obtained with the approximated potential. Using this augmented set of functions, the first iteration is completed by calculating a new T matrix. A second iteration is begun by constructing a new set of solutions and combining them with the initial trial functions set; this will yield a new T matrix. The iterative procedure is continued until the wavefunctions converge, yielding the LSE solutions for the exact potential U ^{229,230}.

This method has been widely used to study PI of molecular systems. Using CGTO as the initial set of functions R , we find calculations by Lucchese *et al*⁴² for N_2 ; using spherical GTOs, Lucchese *et al*^{45,230} calculated PI cross section for CO_2 and Lynch *et al*²³¹ for C_2H_2 . Natalense *et al* presented results for SF_6 ²³² and for CH_4 , CF_4 and CCl_4 ²³³; Machado *et al* for H_2O ²³⁴ and SiH_4 ²³⁵; Machado and Masili²³⁶ studied H_2 ; Stephens and McKoy²³⁷ for OH; Braunstein *et al*²³⁸ for CH_4 ; Wells and Lucchese²³⁹ for C_2H_2 ; for C_{60} we find the results by Gianturco and Lucchese²⁴⁰; and Wiedmann *et al*²⁴¹ calculated the rotationally resolved PI cross section for CH_3 , H_2O , H_2S and H_2CO .

4.12.2 Continued Fractions

The method of continued fractions (MCF) was originally proposed by Horáček et Sasakawa^{242,243} for the study of elastic scattering of fast electrons by atoms; subsequently, Lee *et al* adapted it to study scattering of slow electrons by atoms²⁴⁴ and by linear molecules²⁴⁵, and extended it to study ionization by electron collisions in polyatomic molecules^{246,247}. The extension of the MCF to the PI study of molecules is explained with details in Reference 248. The idea is to represent the scattering matrix as a continued fraction. The continuum wavefunction is obtained from the solution of the LSE using the static-exchange potential, with the long-range Coulomb potential of the ionic core removed. The MCF does not require basis functions and it is characterized by rapid convergence.

The application of the MCF starts with the definition of a n th-order weakened potential operator $U^{(n)}$, from which the reactance matrix \mathbf{K} is expressed in the form of a continued fraction. The n th-order correction to \mathbf{K} , as well as to the wavefunction, can be approximated successively. The operator $U^{(n)}$ becomes weaker and weaker as n increases, and the procedure can be stopped after a few steps. The converged \mathbf{K} matrix corresponds to the exact solution

730 for a given potential U in LSE²⁴⁸.

731 To our knowledge, the MCF has been used only to study PI of NH_3 ²⁴⁸.

732 4.13 Crank–Nicolson

733 The Crank–Nicolson (CN) method²⁴⁹ was originally developed to solve numerically differential equations of heat-conduction type, employing a combination of backward/forward finite-difference of all involved variables. It is correct up to the second order in $\hat{H}\Delta t$, and is numerically stable. The CN scheme can be used to propagate an initial wavefunction with an imaginary time evolution operator, in which, by the Wick rotation, the time t is replaced by $-i\tau$. In such a way, any initial arbitrary state can converge directly to a particular desired state (bound or continuum), just by adjusting the time-step of the propagator.

741 The CN scheme has been used to study general PI features by Goldberg and Shore²⁵⁰; we can find also different studies in PI of H_2^+ by Picón *et al*²⁵¹, Yuan *et al*²⁵², Silva *et al*²⁵³ and Bian²⁵⁴. The ion HeH^{2+} has been studied by Bian²⁵⁴ and the angular distributions for H_2 by Yuan *et al*²⁵².

745 5 Sturmian Approach

746 5.1 Generalized Sturmian Functions

747 In the literature we can find different approaches to Sturmian functions, depending on the type of problem to be solved. There are essentially two lines, one associated to bound states and another to scattering problems. The first line initiated by Shull and Löwdin²⁵⁵, formalized by Goscinski²⁵⁶ and impuled later on by Aquilanti and coworkers^{257,258}. It is within this line that the generalized Sturmian functions were introduced by Avery and coworkers^{259,260} to deal with many electron atoms and chemical systems. On the scattering line, the work was initiated by Rawitscher^{261,262} and continued by Macek, Ovchinnikov and coworkers^{263,264}. We extended the scattering functions proposed by Rawitscher and started to use them in scattering studies with the name Generalized Sturmian Functions (GSFs) to indicate that the basis functions are solving general atomic potentials.

759 Details about the presently used GSF are given in References 22 and 23 and references therein, and only the essentials are recalled here. GSF are solutions of a Sturm-Liouville problem, from which Rotenberg took the name. Noted $\mathcal{S}_n^{(\ell, E)}(r)$, they are regular at the origin and satisfy the two-body non-homogeneous Schrödinger equation

$$764 \left[-\frac{1}{2} \frac{d^2}{dr^2} + \frac{\ell(\ell+1)}{2r^2} + \mathcal{U}(r) - E \right] \mathcal{S}_n^{(\ell, E)}(r) = -\beta_n^{(\ell, E)} \mathcal{V}(r) \mathcal{S}_n^{(\ell, E)}(r), \quad (9)$$

765 where E is an externally fixed parameter and $\beta_n^{(\ell, E)}$ are the eigenvalues for a given angular momentum ℓ . In general, the generating potential $\mathcal{V}(r)$, a short-range potential, dictates the size of the inner region in which most of the dynamics is supposed to occur, while the auxiliary potential $\mathcal{U}(r)$ determines the asymptotic behavior of all GSFs. This property is illustrated in Figure 5.1, for functions with a fixed energy $E = 0.5$ a.u., an auxiliary Coulomb potential with

771 charge $Z = -1$ and a Yukawa generating potential. In general, the outgoing
 772 asymptotic behavior of the GSFs with an auxiliary Coulomb potential is given
 773 by the second term of (3)

$$774 \quad \lim_{r \rightarrow \infty} \mathcal{S}_n^{(\ell, E)}(r) \propto e^{i(kr - \frac{Z}{k} \ln(2kr))}. \quad (10)$$

775 Additionally, all the solutions conform a complete basis set, with the potential-
 776 weighted orthogonality relation

$$777 \quad \int_0^\infty dr \mathcal{S}_{n'}^{(\ell, E)}(r) \mathcal{V}(r) \mathcal{S}_n^{(\ell, E)}(r) = \delta_{n'n}. \quad (11)$$

778 Note that the integral is defined without taking the complex conjugate of the
 779 function $\mathcal{S}_{n'}^{(\ell, E)}(r)$.

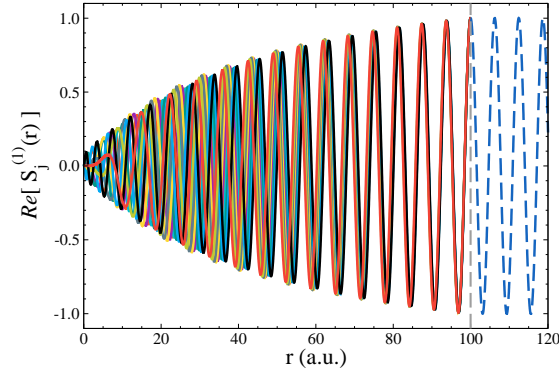


Figure 5.1: (Color online) Real part of 10 generalized Sturmian functions, with a fixed energy $E = 0.50$ a.u. and $\ell = 1$, obtained solving Equation (9), for $r \in [0, 100]$, together with a Coulomb auxiliary potential with charge $Z = -1$, and a Yukawa potential as a generating potential, with parameter $\alpha_{\text{short}} = 0.0219$. The exact Coulomb (analytic) regular function (blue, dash) is also shown.

780 5.2 Sturmian Approach to Photoionization Process

781 We shall present in this section the theoretical formalism developed within a
 782 Sturmian approach for molecules. We start with a brief description of the used
 783 molecular model potentials, then we derive the driven equation of the TISE and
 784 provide the necessary formula to calculate the PI cross section. As a simple
 785 illustration of the numerical implementation in the atomic case, we show results
 786 for the hydrogen atom.

787 5.2.1 Molecular Model Potentials

788 To study PI of molecules, we shall use the SAE approximation²⁶⁵ for the initial
 789 state wavefunction. We then need a molecular model potential that plays the
 790 role of a scattering potential. Consider the active electron placed in the MO
 791 i of the ground state, and denote $\phi_i(\mathbf{r})$ the corresponding wavefunction. The

792 molecular model potential we shall use is the following²⁶⁶

$$793 \quad V_{i \text{ mol}}(\mathbf{r}, \mathbf{R}) = - \sum_{n=1}^M \frac{Z_n}{|\mathbf{r} - \mathbf{R}_n|} + \sum_{j=1}^{N_{\text{MO}}} N_{ij} \int d\mathbf{r}' \frac{|\phi_j(\mathbf{r})|^2}{|\mathbf{r} - \mathbf{r}'|}, \quad (12)$$

794 where M is the number of nuclei in the molecule, Z_n is the charge of each
795 nucleus, \mathbf{R}_n is the position of each nuclei respect to the center of mass of the
796 molecule, N_{MO} is the number of MOs and $N_{ij} = 2 - \delta_{ij}$. This potential is the
797 direct term within the SEA. For the sake of simplicity, the \mathbf{R} dependence is
798 omitted hereafter.

799 We shall take the MO i given by Moccia; they are expressed as

$$800 \quad \phi_i(\mathbf{r}) = \sum_{j=1}^N A_{ij} \mathcal{R}_j(r) S_{\ell_j}^{m_j}(\hat{r}), \quad (13)$$

801 where $S_{\ell_j}^{m_j}(\hat{r})$ are the real spherical harmonics³⁰, and the N radial wavefunc-
802 tions are given as Slater type-orbitals (STOs)

$$803 \quad \mathcal{R}_j(r) = \left[\frac{(2\zeta_j)^{2n_j+1}}{(2n_j)!} \right]^{1/2} r^{n_j-1} e^{-\zeta_j r}, \quad (14)$$

804 with tabulated integers n_j and exponents ζ_j . These MO allow one to calculate
805 analytically, in a partial-wave expansion, the molecular model potential.

806 As mentioned before, in a typical experiment the molecules are randomly
807 oriented. Although this is not the proper way to proceed, we may consider as
808 starting point an angular average of the model potential (12), i.e., a central
809 potential

$$810 \quad U_{i \text{ mol}}(r) = \frac{1}{4\pi} \int_{4\pi} d\hat{r} V_{i \text{ mol}}(\mathbf{r}). \quad (15)$$

811 This averaging procedure is illustrated through Figure 5.2, where the effective
812 charges $rU_{i \text{ mol}}(r)$ and $rV_{i \text{ mol}}(\mathbf{r})$ for two set of angles (θ, ϕ) are compared in the
813 case of CH_4 . The effective charge goes from -6 at $r = 0$ and to -1 asymptoti-
814 cally. The minimum is located at $r \approx 2.08$ a.u., i.e. at the equilibrium position
815 of each H atom; its depth and sharpness depend on the orientation and whether
816 the angular average has been performed or not.

817 The model potential (12) proposed in this work can be certainly improved
818 in many aspects, some of which are under current investigation. One of them is
819 the inclusion of the exchange. Also, as we use an independent particle approxi-
820 mation, some many-body aspects (i.e., correlation) are only included indirectly
821 through the use of MO in Equation (12), but not explicitly.

822 5.2.2 Driven Equation and Cross Section

823 To introduce our Sturmian approach, we start with the use of an arbitrary
824 potential $U(\mathbf{r})$, such as the one given by Equation (12). We describe the PI
825 process using the first-order perturbation theory for a molecule that interacts
826 with a radiation field. The Hamiltonian can be written as

$$827 \quad \widehat{\mathcal{H}} = \widehat{H}_0 + \widehat{W}(t), \quad (16)$$

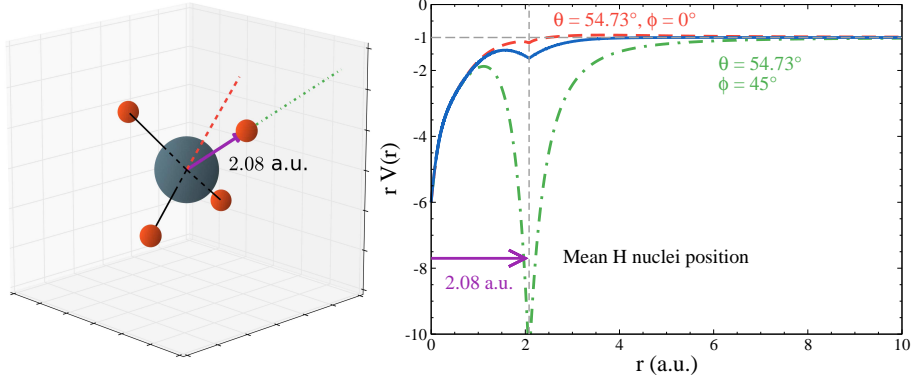


Figure 5.2: (Color online) **Left panel:** Representation of the spatial localization of the individual atoms on CH_4 ; the mean equilibrium distance is indicated. **Right panel:** Molecular model (12) (red dash and green dash-dot) and angular averaged (15) (blue, solid) potentials for CH_4 , at indicated angles. The potential in green (dash-dot) corresponds to the variation of the potential on the the green path on the figure of the left panel.

828 where $\hat{H}_0 = \hat{T} + U(\mathbf{r}, \hat{\mathfrak{R}})$ is the field-free Hamiltonian of the target with
 829 $\hat{\mathfrak{R}} = (\alpha, \beta, \gamma)$ the set of Euler angles that specify the spatial orientation of
 830 the molecule; \hat{T} is the kinetic energy operator, and

$$831 \quad \widehat{W}(t) = \begin{cases} -F^{(L)}(t) \hat{\mathbf{e}} \cdot \mathbf{r} = F(t) \widehat{D}^{(L)}, & \text{length gauge} \\ -F^{(V)}(t) \hat{\mathbf{e}} \cdot \mathbf{p} = F(t) \widehat{D}^{(V)}, & \text{velocity gauge} \end{cases} \quad (17)$$

832 where $F^{(g)}(t)$ is the electric field in the length gauge or the vector potential in
 833 the velocity gauge, $\hat{\mathbf{e}}$ gives the polarization of the field and \widehat{D} are the dipolar
 834 operators (2); $F(t)$ contains the time-dependent profiles of the radiation field.

835 Dropping the explicit $\hat{\mathfrak{R}}$ -dependence for the moment, we begin with the
 836 TDSE for the total Hamiltonian (16)

$$837 \quad \left(i \frac{\partial}{\partial t} - \hat{\mathcal{H}} \right) \Psi(\mathbf{r}, t) = \left(i \frac{\partial}{\partial t} - \hat{H}_0 - \widehat{W}(t) \right) \Psi(\mathbf{r}, t) = 0, \quad (18)$$

838 and propose the general solution to be

$$839 \quad \Psi(\mathbf{r}, t) = e^{-i\omega_0 t} \left[\Phi^{(0)}(\mathbf{r}) + \Psi_{\text{scatt}}(\mathbf{r}, t) \right], \quad (19)$$

840 where $\Phi^{(0)}(\mathbf{r})$ is the wavefunction of the initial ground state of the molecule,
 841 usually the active MO to ionize, with energy ω_0 , and $\Psi_{\text{scatt}}(\mathbf{r}, t)$ is the wavefunc-
 842 tion of the photoelectron, with energy $\omega = E$ (in atomic units). Replacing (19)
 843 in (18), we obtain

$$844 \quad \left[i \frac{\partial}{\partial t} - \omega_0 - \hat{H}_0 - \widehat{W}(t) \right] \Psi_{\text{scatt}}(\mathbf{r}, t) = \widehat{W}(t) \Phi^{(0)}(\mathbf{r}). \quad (20)$$

845 Now, if we apply a Fourier transform to (20), we obtain the TISE

$$846 \begin{aligned} (\omega - \omega_0 - \widehat{H}_0) \Psi_{\text{scatt}}(\mathbf{r}, \omega) - \frac{1}{\sqrt{2\pi}} \int_{-\infty}^{\infty} d\omega' \widehat{\mathcal{W}}(\omega') \Psi_{\text{scatt}}(\mathbf{r}, \omega - \omega') \\ = \widehat{\mathcal{W}}(\omega) \Phi^{(0)}(\mathbf{r}), \end{aligned} \quad (21)$$

847 where $\widehat{\mathcal{W}}(\omega)$ is the Fourier transform of $\widehat{\mathcal{W}}(t)$.

848 Equation (21) contains the interaction with the field to all orders, and there-
849 fore $\Psi_{\text{scatt}}(\mathbf{r}, \omega)$ contains information over all possible processes. Neglecting the
850 integral term of (21), we can introduce a perturbative expansion on the scat-
851 tering wavefunction²⁵. Since we are interested here only in single PI processes,
852 we retain the first order, and then Equation (21) results in the driven equation
853 for the final state wavefunction

$$854 (\omega - \omega_0 - \widehat{H}_0) \Psi^{(1)}(\mathbf{r}, \omega) = \widehat{\mathcal{W}}(\omega) \Phi^{(0)}(\mathbf{r}). \quad (22)$$

855 This is the equation that we want to solve; the scattering wavefunction at first
856 order, $\Psi^{(1)}(\mathbf{r}, \omega)$, will provide the PI information.

857 To solve equation (22), we separate first the scattering wavefunction in its
858 radial and angular parts

$$859 \Psi^{(1)}(\mathbf{r}, \omega) = \frac{1}{r} \sum_{\ell m} \varphi_{\ell}(r, \omega) Y_{\ell}^m(\hat{r}). \quad (23)$$

860 Usually, the radial wavefunction $\varphi_{\ell}(r, \omega)$ is expanded in some radial basis set.
861 Within our Sturmian approach it is expanded in a GSF set (see Section 5.1)

$$862 \varphi_{\ell}(r, \omega) = \sum_j a_j^{(\ell, E)}(\omega) \mathcal{S}_j^{(\ell, E)}(r). \quad (24)$$

863 Performing an angular projection, Equation (22) is converted into a set of
864 angular-coupled differential equations

$$865 \sum_{\ell m} \left[\left(\omega - \omega_0 + \frac{1}{2} \frac{d^2}{dr^2} - \frac{\ell(\ell+1)}{2r^2} \right) \delta_{\ell' \ell} \delta_{m' m} - U_{\ell' \ell}^{m' m}(r) \right] \varphi_{\ell}(r, \omega) = \varrho_{\ell'}^{m'}(r, \omega), \quad (25)$$

866 where $U_{\ell' \ell}^{m' m}(r) = \langle \ell' m' | U(\mathbf{r}) | \ell m \rangle$ and $\varrho_{\ell'}^{m'}(r, \omega) = r \langle \ell' m' | \widehat{\mathcal{W}}(\omega) | \Phi^{(0)} \rangle$. As
867 mentioned in Section 1, the use of a non-central potential to describe the molec-
868 ular target couples directly the different angular momenta of the initial state.
869 For atoms or angular averaged molecular potentials, on the other hand, there is
870 no coupling, $U_{\ell' \ell}^{m' m}(r)$ is diagonal and we have a single radial equation

$$871 \left(\omega - \omega_0 + \frac{1}{2} \frac{d^2}{dr^2} - \frac{\ell(\ell+1)}{2r^2} - U(r) \right) \varphi_{\ell}(r, \omega) = \varrho_{\ell}^m(r, \omega). \quad (26)$$

872 Recall now that the potential $U(\mathbf{r}, \hat{\mathfrak{R}})$ of the field-free Hamiltonian \widehat{H}_0 con-
873 tains the orientation $\hat{\mathfrak{R}}$ of the molecule. This orientation dependence is to be
874 accounted for by $\varphi_{\ell}(r, \omega)$ and finally by the coefficients $a_j^{(\ell, E)}(\omega)$, so that we
875 actually have $a_j^{(\ell, E)}(\omega, \hat{\mathfrak{R}})$.

876 Now, to solve the coupled system of Equations (25), we use the GSF expansion
877 (24), and obtain

$$878 \sum_{\ell m} \sum_j \left[\left(\omega - \omega_0 + \frac{1}{2} \frac{d^2}{dr^2} - \frac{\ell(\ell+1)}{2r^2} \right) \delta_{\ell'\ell} \delta_{m'm} - U_{\ell'\ell}^{m'm}(r) \right] \\ \times a_j^{(\ell, E)}(\omega) \mathcal{S}_j^{(\ell, E)}(r) = \varrho_{\ell'}^{m'}(r, \omega). \quad (27)$$

879 The final step consists in projecting (27) on $\mathcal{S}_i^{(\ell, E)}(r)$ (note that it is not the
880 complex conjugate, see Equation (11)): then, all the resulting matrices are
881 calculated as indicated in References 22 and 23. Solving the matricial problem
882 with standard numerical methods provides the coefficients $a_j^{(\ell, E)}(\omega)$.

883 All GSFs of the basis set have the same and correct asymptotic behavior,
884 in this case the behavior dictated by the Coulomb potential (see Section 5.1).
885 This means that our basis functions possess, by construction, important phys-
886 ical information and need to expand essentially the inner region, whose size
887 will be determined by the range of the driven term. This makes the basis set
888 adequate and finally computationally efficient. From the asymptotic property
889 of the GSFs, we obtain the transition amplitude directly from the expansion
890 coefficients of the scattering wavefunction in (24)²⁶⁷

$$891 \mathcal{T}(\omega, \hat{r}, \hat{\mathfrak{R}}) = -\sqrt{2\pi} \sum_{\ell} Y_{\ell}^m(\hat{r}) \langle \Psi_{-\mathbf{k}}^{(-)} | \widehat{\mathcal{W}}(\omega) | \Phi^{(0)} \rangle = \sum_{\ell m j} Y_{\ell}^m(\hat{r}) a_j^{(\ell, E)}(\omega, \hat{\mathfrak{R}}). \quad (28)$$

892 After an angular projection, we finally have the PI cross section as a function
893 of the photon energy²⁶⁷

$$894 \frac{d\sigma^{(\ell)}(\hat{\mathfrak{R}})}{dE} = \frac{4\pi^2 \omega_{ki}^{(g)}}{c} k \frac{1}{2\pi} \frac{|\sum_j a_j^{(\ell, E)}(\omega, \hat{\mathfrak{R}})|^2}{|\mathcal{F}(\omega)|^2}. \quad (29)$$

895 where $\omega^{(L)} = E - E_0$ or $\omega^{(V)} = (E - E_0)^{-1}$ is the difference between final and
896 initial energies in either length or velocity gauges, and $\mathcal{F}(\omega)$ is the Fourier
897 transform of the radiation field profile $F(t)$.

898 5.2.3 Example: Hydrogen Atom

899 The coupled system of equations (27) allows us to study PI processes for any po-
900 tential. For systems that are described with a central potential, we are left with
901 a single differential equation^{267,268}. Applications to a set of different molecules
902 will be given in Section 5.3 and is here illustrated for hydrogen atom. For this
903 atomic target, we solved the TISE (27) in both length and velocity gauges for
904 electron energies in the range [0.00, 3.00]. Each one of these energies was used
905 as the fixed energy E to calculate our GSFs basis through (9), where a Coulomb
906 potential with charge -1 was taken as auxiliary potential and a Yukawa poten-
907 tial with an energy-dependent parameter as generating potential. For the initial
908 state we used the exact ground state wavefunction of the atom. Our calculated
909 PI cross section (29) is shown in Figure 5.3, and is compared with the analytical
910 formula given by Harriman²⁶⁹. Agreement between the cross sections in both
911 gauges is perfect. Comparing with the analytical formula we obtain errors of the
912 order of $10^{-8} \sim 10^{-11} \%$ over all the energy range (see Figure 5.4), showing that

913 our results with the selected GSF parameters gives very stable and “numerically
914 exact” solutions to the TISE (22).

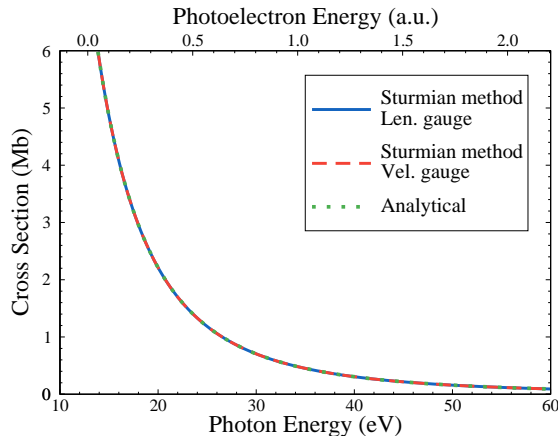


Figure 5.3: (Color online) PI cross section of H atom from the ground state $1s$, in Mb versus photon energy in eV. Our results for length (blue, solid) and velocity (red, dash) and are compared with the exact analytical formula by Harriman²⁶⁹ (green, dots).

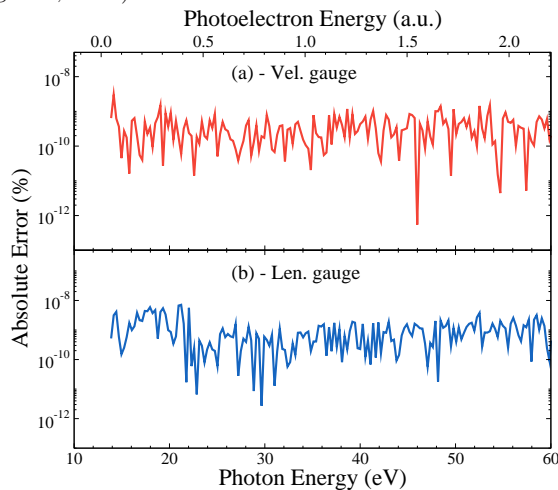


Figure 5.4: (Color online) Absolute errors for the calculated PI cross section in Figure 5.3. (a): For the results in velocity gauge and (b): in length gauge.

915 5.3 Results For Molecules

916 In this section we report some results obtained by applying our Sturmian approach for molecular single PI, first solving Equation (27) for the angular averaged potential (15), and then using the non-central potential (12). Some results
917 have been partially published before^{268,270} for CH_4 and H_2O . The treatment
918 of molecular systems with an averaged (central) potential is similar to that of
919 atomic systems. For all cases we used 60 GSFs for each final energy and final
920
921

922 (ℓ, m) set; the basis functions are defined in a box of 50 a.u., using an aux-
923 iliary Coulomb potential with charge -1 , and a generating Yukawa potential
924 with an energy-dependent parameter. We have verified that in all cases the
925 cross sections are converged in terms of number of GSFs. The initial MO were
926 taken from Moccia publications, specifically for H_2O from Reference 271, for
927 NH_3 from Reference 272 and for CH_4 from 273. For the non-central potential,
928 with the fixed spatial molecular orientation given by Moccia, we use exactly the
929 same GSF basis and initial MOs. The respective PI cross sections were calcu-
930 lated using Equation (29), and we shall present our results in both length and
931 velocity gauges. It is worth emphasizing here that the majority of theoretical
932 publications on molecular PI present results obtained with the length gauge,
933 but do not provide a detailed analysis of gauge agreement, as it is often done
934 for atomic systems.

935 5.3.1 H_2O

936 First, we start to study PI from the valence orbitals of H_2O whose electronic
937 ground state configuration is $1a_1^2 2a_1^2 1b_2^2 3a_1^2 1b_1^2 {}^1A_1$. We study here only the
938 two valence MOs. For the inner valence orbital $3a_1$ ($E_0 = -15.1323$ eV), the
939 calculated PI cross sections are shown in Figure 5.5, and for the outer orbital
940 $1b_1$ ($E_0 = -13.4805$ eV) in Figure 5.6. Both are compared with TD-DFT
941 calculations by Stener *et al*⁹¹, GIPM/D by Kilcoyne *et al*¹⁵⁵, STT by Cacelli
942 *et al*¹⁹⁹, and ISM by Machado *et al*²³⁴; the experimental data were reported
943 by Banna *et al*²⁷⁴.

944 For the MO $3a_1$, we observe a good agreement between our results in veloc-
945 ity gauge and other theoretical calculations, in particular for photon energies
946 beyond 30 eV, where our results are very close to the TD-DFT and GIPM/D;
947 on the other hand, the length gauge results considerably overestimate the cross
948 sections for all calculated energies. In general, the cross sections for inner val-
949 ence orbitals are difficult to calculate accurately, due to the presence of different
950 many-body effects, as relaxation of the core.

951 For the MO $1b_1$, the gauge discrepancy is of the same order as for the $3a_1$
952 case. Our cross sections compare fairly with other theoretical results, ours being
953 seemingly too low in the threshold region where unfortunately no experimental
954 data are available.

955 The results obtained using the non-central potential (12), are only slightly
956 better, indicating therefore that the central potential (15) is good enough to
957 study this particular molecule.

958 5.3.2 NH_3

959 Next we study PI for both valence orbitals of NH_3 whose ground state electronic
960 structure is $1a_1^2 2a_1^2 1e^4 3a_1^2 {}^1A_1$. For the inner valence MO $1e$ ($E_0 = -16.2071$
961 eV), the cross section is shown in Figure 5.7, and for the outer valence MO $3a_1$
962 ($E_0 = -11.2819$ eV) in Figure 5.8. Our results are compared with the TD-DFT
963 results by Stener *et al*⁹¹, GIPM/D by Kilcoyne *et al*¹⁵⁵, STT by Cacelli *et al*¹⁹⁹,
964 and with calculations using MCF by Nascimento *et al*²⁴⁸; the experimental data
965 were reported by Brion *et al*²⁷⁵.

966 For the orbital $1e$, our results in velocity gauge show only a fair agreement
967 with all reported data, in particular at high photon energies. Gauge discrepancy

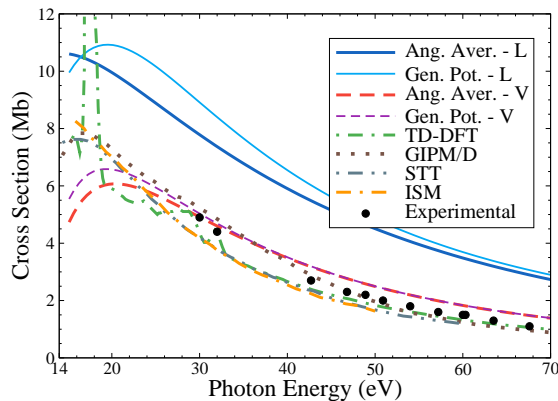


Figure 5.5: (Color online) Partial PI cross section in Mb versus photon energy in eV from the MO $3a_1$ of H_2O . Our results using the angular averaged molecular potential (15) for length (blue, solid) and velocity (red, dash) gauges, and using the non-central potential (12) in length (light blue, thin solid) and velocity (purple, thin dash) gauges are compared with results for TD-DFT⁹¹ (green, dash-dot); GIPM/D¹⁵⁵ (brown, dots); STT¹⁹⁹ (gray, dash-dot-dot); ISM²³⁴ (orange, dash-dash-dot) and with experimental data²⁷⁴ (black dots).

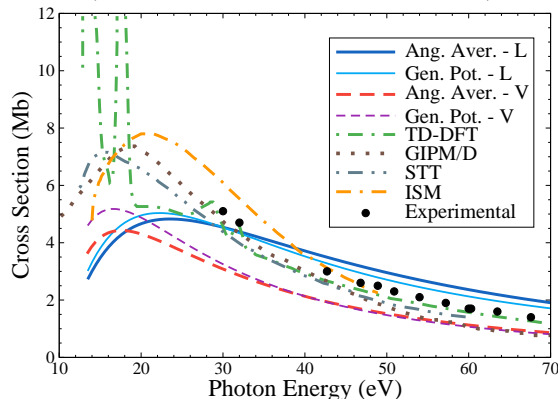


Figure 5.6: (Color online) Same as Figure 5.5 for MO $1b_1$ of H_2O .

968 is again important and, fortuitously, the length gauge results reproduce the
969 experimental magnitude around 22 eV.

970 For the orbital $3a_1$, our results exhibit a slightly better gauge agreement;
971 the length gauge cross section presenting the same shape, but with a larger
972 magnitude. The results in velocity gauge are in acceptable agreement with the
973 experimental data over the whole energy range.

974 As for H_2O , the use of the non-central potential (12) has a small effect,
975 except in length gauge for the $3a_1$ orbital.

976 5.3.3 CH_4

977 Finally, we show our results for CH_4 whose ground state electronic structure is
978 $1a_1^2 2a_1^2 1t_2^6 {}^1A_1$. The calculated PI cross sections in both length and velocity
979 gauges for the inner valence MO $2a_1$ ($E_0 = -25.0454$ eV) are shown in Fig-

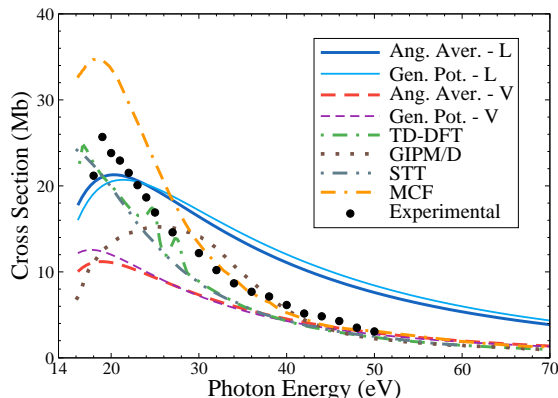


Figure 5.7: (Color online) Partial PI cross section in Mb versus photon energy in eV from the MO $1e$ of NH_3 . Our results using the angular averaged potential (15) for length (blue, solid) and velocity (red, dash) gauges, and using the non-central (12) in length (light blue, thin solid) and velocity (purple, thin dash) gauges, are compared with results for TD-DFT⁹¹ (green, dash-dot); GIPM/D¹⁵⁵ (brown, dots); STT¹⁹⁹ (gray, dash-dot-dot); MCF²⁴⁸ (orange, dash-dash-dot) and with experimental data²⁷⁵ (black dots).

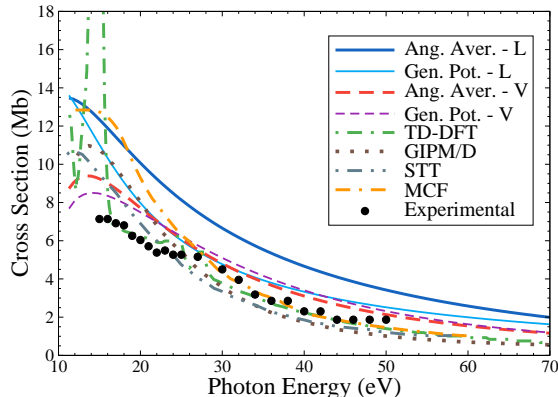


Figure 5.8: (Color online) Same as Figure 5.7 for the MO $3a_1$ of NH_3 .

980 ure 5.9, and for the outer valence MO $1t_2$ ($E_0 = -13.7199$ eV) in Figure 5.10.
 981 They are compared with TD-DFT calculations by Stener *et al*⁹¹, GIPM/D by
 982 Kilcoyne *et al*¹⁵⁵, MSM by Rosi *et al*¹³², and with STT by Cacelli *et al*²⁰⁰; the
 983 experimental data are taken from Backx and van der Wiel²⁷⁶.

984 For the inner valence orbital $2a_1$, the length gauge calculation shows no
 985 agreement with any other calculations. For higher energies, say beyond 40 eV,
 986 we have a good agreement between our velocity results and experimental and
 987 other theoretical data.

988 For outer valence orbital $1t_2$, results obtained in velocity gauge show a fair
 989 agreement with experimental data, at least for photon energies higher than 30
 990 eV; near threshold the position of the experimental peak is rather well repro-
 991 duced but not its magnitude. Length gauge results are about a factor two too
 992 large.

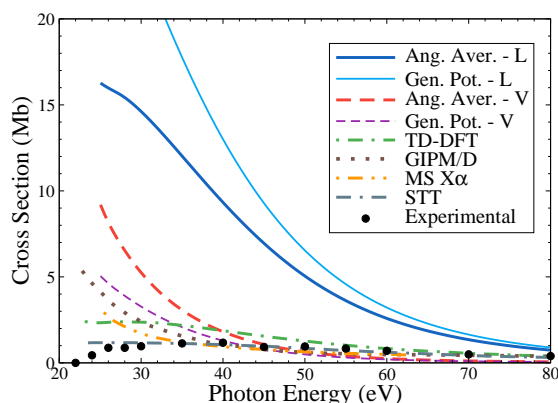


Figure 5.9: (Color online) Partial PI cross section in Mb versus photon energy in eV from the MO $2a_1$ of CH_4 . Our results using the central potential (15) for length (blue, solid) and velocity (red, dash) gauges, and using the non-central (12) for length (light blue, thin solid) and velocity (purple, thin dash) gauges, are compared with TD-DFT⁹¹ (green, dash-dot); GIPM/D¹⁵⁵ (brown, dots); MSM¹³² (orange, dash-dot-dot); STT²⁰⁰ (gray, dash-dash-dot) and with experimental data²⁷⁶ (black dots).

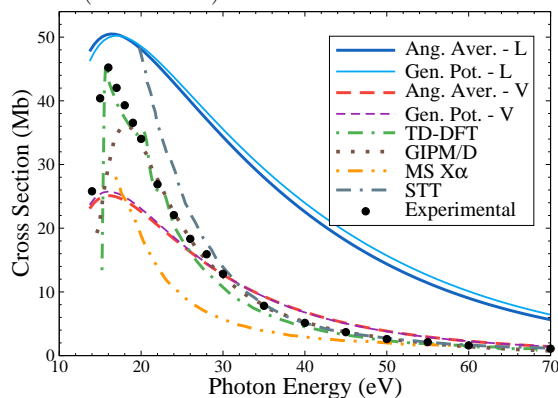


Figure 5.10: (Color online) Same as Figure 5.9 for the MO $1t_2$ of CH_4 .

993 For this molecule, the effect of using the non-central potential (12) is almost
 994 unnoticeable for the $1t_2$ orbital but improves the velocity gauge result for the
 995 $2a_1$ orbital at lower energies.

996 As can be observed from Figures 5.5 to 5.10, the Sturmian approach can
 997 give reasonable PI cross sections, in particular for ionization from the outer
 998 MOs. Some general features are: (i) little difference is seen between the use of
 999 the angular averaged (central) potential (15) and the non-central potential (12)
 1000 (the latter improves marginally the cross sections); (ii) the length gauge results
 1001 are systematically much larger over the whole energy range than those obtained
 1002 with the velocity gauge, and are generally not in agreement with other data
 1003 (experimental or theoretical). This discrepancy indicates that the initial state
 1004 description needs to be improved; (iii) our velocity gauge results are in overall
 1005 fair agreement with other theoretical cross sections, in particular for energies

1006 above, say, 15 – 20 eV over the ionization threshold; (iv) exactly as illustrated
1007 in Section 3 with other molecules, the agreement between theoretical results
1008 (including ours) and experimental data is not uniform. For energies below 15
1009 eV above ionization threshold agreement is generally poor.

1010 6 Conclusions

1011 In this contribution we explored different theoretical aspects of PI of molecules.
1012 The description of this process requires solving quantum mechanically a very
1013 difficult many-body and multi-center problem. Contrary to molecular electronic
1014 structure calculations, one needs to evaluate a continuum state with appropriate
1015 asymptotic conditions. To make calculations feasible, a number of approxima-
1016 tions has to be made. Moreover, over the years, a range of theoretical methods
1017 and numerical techniques have been proposed. Among them, one finds those
1018 familiar in quantum chemistry such as HF, CI and DFT, but also others, such
1019 as the RMM, CS or RPA, which encountered great success in atomic scattering
1020 calculations and were extended to molecular targets. Since in most experiments
1021 the molecules are randomly oriented, an average of the cross sections must be
1022 performed over all spatial orientations. This is an extra computational challenge
1023 that does not appear when studying collisions with atomic targets.

1024 We began (Section 3) by describing the degree of theoretical-experimental
1025 agreement one may find in the literature. The PI of the valence orbitals of
1026 H_2 , N_2 , CO_2 and C_6H_6 , are taken as an illustration, and allow to pinpoint
1027 some of the challenges one is confronted to. Except for H_2 , a non-uniform
1028 picture arises. Agreement between theoretical results and experimental data is
1029 not always satisfactory; moreover, depending on the molecular orbital which is
1030 ionized and the energy range, severe discrepancies are often observed between
1031 different calculations. This is due to both the approximations made and the
1032 technique adopted. For this reason we provided, in Section 4, a brief description
1033 of each method, together with the list of molecules to which they are applied.

1034 We then introduced (Section 5) our Sturmian approach for PI. Essentially,
1035 the method provides one-electron basis functions (named Generalized Sturmian
1036 Functions) with adequate asymptotic boundary conditions. As they intrinsically
1037 contain this property, the basis functions are particularly adequate in describing
1038 the ionized electron continuum state. We briefly described how the Sturmian
1039 method, developed originally for atoms, may be implemented for molecules with
1040 a non-central molecular potential.

1041 As indicated above, in order to reduce the complexity of the problem, differ-
1042 ent approximations must be considered to make it tractable. In this very first
1043 implementation of the Sturmian approach we started with the OCE and the
1044 SAE approximations. These reduce considerably the dimension of the problem
1045 and allow one to deal with one-electron wavefunctions, an ideal starting point
1046 to test the versatility of our method for molecules. It is well known that these
1047 approximations are good enough to study symmetric molecules, and in particu-
1048 lar the ones with a heavy nucleus in its center of mass; this is the case for
1049 the selected molecules in this work (H_2O , NH_3 and CH_4) for which we reported
1050 results for PI from their valence orbitals. We stress here that the computational
1051 procedure to obtain such results is exactly the same as the one used to study
1052 PI in hydrogen atom, with an angular averaged molecular model potential (15).

1053 The same GSF basis and initial state wavefunctions are used for calculations
1054 with the non-central potential (12). It turns out that the use of the latter only
1055 slightly improves the calculated cross sections. A systematic gauge comparison
1056 clearly showed that the length gauge largely overestimates the spectra at all
1057 energies. Considering some of the crude approximations, we may state that the
1058 implemented technique yields velocity gauge cross sections in reasonable agree-
1059 ment with experimental data, in particular at higher photoelectron energies.
1060 Although clearly perfectible (see below), these results are promising since they
1061 demonstrate that we have a working computational tool to study the electronic
1062 spectra of different molecules.

1063 Let us add a short comment on computational efficiency. As illustrated
1064 by several bound-state calculations reported in our review²² (and references
1065 therein), the GSF method is able to deliver results with high accuracy and low
1066 computational cost. For scattering calculations, although there is not a rigorous
1067 way to perform efficiency comparisons, some estimations were given in Reference
1068 277 with studies of three-body atomic breakup problems. Comparisons between
1069 the GSF and state-of-the-art methods proved that our methodology improves
1070 the numerical efficiency by at least an order of magnitude. Recently, in a study
1071 of DPI of He²⁷⁸, the GSF method reproduced very precisely ECS differential
1072 cross sections with a substantial gain (more than 50%) in memory storage of
1073 Hamiltonian matrix. In the present molecular applications the GSF tool is
1074 similar. The built in properties make the GSF set very adequate (and, to our
1075 mind, efficient) to deal with scattering problems, here PI.

1076 The use of the angular averaged molecular model potential, which is equiv-
1077 alent to include the random orientation of the molecule before the scattering
1078 calculations, gave us good results for high energies; for lower energies a better
1079 description of the target is clearly necessary. Besides the molecular potential
1080 itself, in that regime all the many-body effects are important, and the wave-
1081 function for the initial state should include all active electrons. In that respect,
1082 we tried to include exchange terms in different manners. In our preliminary
1083 attempts, such terms did not remove the observed gauge discrepancies; we are
1084 currently investigating other ways to include in our model both exchange and
1085 correlations effects. Furthermore, the interactions with all nuclei becoming im-
1086 portant, a many-center wavefunction should be employed; this may lead in a
1087 very expensive description of the system from the computational point of view,
1088 particularly for polyatomic molecules. The use of a non-central molecular po-
1089 tential (12) gives slightly better results in the low photon energy regime, since
1090 it is a more realistic description of the molecule. However, in this case the cross
1091 sections must be calculated for any Euler angles set. The final angular average
1092 over all possible spatial orientations of the molecule in the laboratory frame (de-
1093 fined by the polarization of the radiation field) is then computationally much
1094 more expensive. Moreover, in all investigated systems, in particular for inner
1095 valence orbitals, we saw that our length gauge results are always overestimating
1096 experimental data. The gauge discrepancies are known (see, for instance, Ref-
1097 erences 89, 199, 200, 202, 268 or 279), but are rarely discussed in the literature
1098 for molecular cases. They can be related to the quality of the wavefunctions for
1099 the initial state and also by the absence of different many-body effects. In order
1100 to obtain a better gauge agreement, one would need to use more sophisticated
1101 wave functions and avoid the FC and SAE approximations, since in some cases
1102 the relaxation effects are important, as it has been shown by TD-DFT results

1103 (see Sections 3, 4.3.2 and Figures 5.6 and 5.10).

1104 As a summary, we have presented here some results of a first implementation
 1105 of our Sturmian approach to study PI of molecules. Improvements of calculated
 1106 cross sections may be obtained using more realistic molecular potentials and
 1107 initial wavefunctions. Investigations in this direction are under way and will be
 1108 presented elsewhere. GSFs offer also a promising tool to study other ionization
 1109 processes in molecular systems such as the single ionization by electron impact,
 1110 the so-called ($e, 2e$) process.

1111 Acknowledgments

1112 We acknowledge the CNRS (PICS project No. 06304) and CONICET (project
 1113 No. DI 158114) for funding our French-Argentinian collaboration, and CON-
 1114 ICET (PIP 201301/607). G. Gasaneo also thanks the support by PGI (24/F059)
 1115 of the Universidad Nacional del Sur.

1116 A List of Photoionization Calculations for Dif- 1117 ferent Molecules

1118 We list here, molecule by molecule, the references of all applications of theoret-
 1119 ical methods mentioned in Section 4.

| | | | |
|------|---|------|--|
| 1120 | Homonuclear diatomic | 1139 | 11. HeH ⁺ ^{58,169} |
| 1121 | 1. H ₂ ⁺ ^{108,109,114,115,118,211,213,254} | 1140 | 12. LiH ¹⁸³ |
| 1122 | ²⁵¹⁻²⁵³ | 1141 | 13. CH ¹⁹⁴ |
| 1123 | 2. H ₂ ^{27,32,33,35,36,57,59,60,75,76} | 1142 | 14. OH ²³⁷ |
| 1124 | ^{110-112,116,118,121,128,145-147} | 1143 | 15. HF ^{77,82,91,148,153,188,200} |
| 1125 | ^{150,153,154,164,165,167,168,176-178} | 1144 | 16. CN ⁻ ¹⁷¹ |
| 1126 | ^{195,217,236,252} | 1145 | 17. CO ^{34,40,44,51,67,71,92,93,101,102} |
| 1127 | 3. D ₂ ^{27,165} | 1146 | ^{128,131,146,148-151,171,203,219} |
| 1128 | 4. Li ₂ ⁶⁸ | 1147 | 18. NO ^{121,170} |
| 1129 | 5. C ₂ ¹ | 1148 | 19. HCl ^{54,82,201} |
| 1130 | 6. N ₂ ^{38-42,51,67,89,101,121} | 1149 | Polyatomic |
| 1131 | ^{117,128,129,131,145-149,151} | 1150 | 20. BH ₃ ⁸² |
| 1132 | ^{153,154,170,171,174,175,179-181,185} | 1151 | 21. H ₂ O ^{82,91,146,148-151,154,155,171} |
| 1133 | ^{193,217} | 1152 | ^{188,196-199,234,241,268} |
| 1134 | 7. O ₂ ⁶⁵ | 1153 | 22. NH ₃ ^{82,91,149,155,171,188,199,220,248} |
| 1135 | 8. F ₂ ²⁰⁴ | 1154 | 23. LiCN ⁶² |
| 1136 | 9. Cl ₂ ⁸⁴ | 1155 | 24. AlH ₃ ⁸² |
| 1137 | Heteronuclear diatomic | | |
| 1138 | 10. HeH ²⁺ ²⁵⁴ | | |

| | | | |
|------|---|------|--|
| 1156 | 25. H ₂ S ^{82,146,149,182,202,241} | 1182 | 49. H ₂ CO ²⁴¹ |
| 1157 | 26. PH ₃ ^{82,89,149} | 1183 | 50. C ₂ H ₂ ^{39,94,98,151,171,181,184,231,239} |
| 1158 | 27. SiH ₄ ^{82,134,235} | 1184 | 51. C ₂ H ₄ ^{50,98,130,145,146,150,171} |
| 1159 | 28. CO ₂ ^{41,44-46,53,69,121,131,171,230} | 1185 | 52. C ₂ H ₆ ¹⁷¹ |
| 1160 | 29. NO ₂ ^{41,44,70,171} | 1186 | 53. C ₂ (CN) ₂ ¹⁴⁸ |
| 1161 | 30. NO ₂ ⁻ ¹⁷¹ | 1187 | 54. C ₃ H ₆ O (methyl-oxirane) ⁸⁶ |
| 1162 | 31. O ₃ ⁵⁵ | 1188 | 55. C ₃ H ₈ ¹⁷¹ |
| 1163 | 32. C ₂ N ₂ ^{41,148} | 1189 | 56. (CH ₃) ₂ S ¹⁴⁹ |
| 1164 | 33. CaHN ¹⁴⁸ | 1190 | 57. C ₄ H ₆ ⁶³ |
| 1165 | 34. C ₂ O ₂ ⁸⁴ | 1191 | 58. C ₄ H ₄ O (furan) ¹⁴⁸ |
| 1166 | 35. COS ¹³¹ | 1192 | 59. C ₄ H ₅ N (pyrrole) ¹⁴⁸ |
| 1167 | 36. NF ₃ ¹³⁸ | 1193 | 60. C ₄ H ₄ N ₂ (pyrimidine) ⁹⁷ |
| 1168 | 37. CS ₂ ^{49,131} | 1194 | 61. C ₄ H ₄ N ₂ (pyrazine) ⁹⁷ |
| 1169 | 38. CF ₄ ^{95,96,132,233} | 1195 | 62. C ₄ H ₄ N ₂ O ₂ (uracil) ⁸⁷ |
| 1170 | 39. PF ₃ ^{135,138} | 1196 | 63. C ₆ H ₆ (benzene) ^{48,50,51,85,205} |
| 1171 | 40. CF ₃ Cl ¹³⁷ | 1197 | 64. C ₆ F ₆ ¹⁴⁹ |
| 1172 | 41. SiF ₄ ¹³⁴ | 1198 | 65. C ₄ F ₄ N ₂ ¹⁴⁸ |
| 1173 | 42. SF ₆ ^{41,221,232} | 1199 | 66. Cr(CO) ₆ ^{41,84} |
| 1174 | 43. CCl ₄ ²³³ | 1200 | 67. C ₁₀ H ₈ (naphthalene) ⁸⁵ |
| 1175 | 44. SiCl ₄ ^{133,134} | 1201 | 68. C ₁₄ H ₁₀ (anthracene) ⁸⁵ |
| 1176 | 45. TiCl ₄ ⁴¹ | 1202 | 69. C ₁₆ H ₁₀ (pyrene) ⁸⁵ |
| 1177 | Organic molecules | 1203 | Fullerenes |
| 1178 | 46. CH ₃ ²⁴¹ | 1204 | 70. C ₂₀ ¹⁸⁷ |
| 1179 | 47. CH ₄ ^{66,82,91,132,145-147,149-151} | 1205 | 71. C ₆₀ ⁺ ¹⁸⁶ |
| 1180 | ^{155,171,188,200,233,238,268,270} | 1206 | 72. C ₆₀ ^{99,187,240} |
| 1181 | 48. CH ₃ I ¹³⁶ | | |

1207 **Bibliography**

- 1208 [1] Padial, N. T.; Collins, L. A.; Schneider, B. I. *Astrophys. J.* **1985**, 298, 369.
1209 [2] Liedahl, D. A.; Paerels, F. *Astrophys. J.* **1996**, 468, L33.
1210 [3] Bautista, M. A.; Romano, P.; Pradhan, A. K. *Astrophys. J. Suppl. Ser.* **1998**, 118,
1211 259.
1212 [4] Dopita, M. A.; Meatheringham, S. J. *Astrophys. J.* **1991**, 367, 115.

- 1213 [5] García-Segura, G.; Langer, N.; Rożyczka, M.; Franco, J. *Astrophys. J.* **1999**, *517*,
1214 767.
- 1215 [6] Monteiro, H.; Schwarz, H. E.; Gruenwald, R.; Heathcote, S. *Astrophys. J.* **2004**, *609*,
1216 194.
- 1217 [7] Mallard, G.; Miller, J. H.; Smyth, K. C. *J. Chem. Phys.* **1982**, *76*, 3483.
- 1218 [8] Robb, D. B.; Blades, M. W. *Anal. Chim. Acta* **2008**, *627*, 34.
- 1219 [9] Levine, J. S.; Javan, A. *Appl. Phys. Lett.* **1973**, *22*, 55.
- 1220 [10] Killian, T. C.; Kulin, S.; Bergeson, S. D.; Orozco, L. A.; Orzel, C.; Rolston, S. L.
1221 *Phys. Rev. Lett.* **1999**, *83*, 4776.
- 1222 [11] Amusia, M. Y.; Baltenkov, A. S. *Phys. Rev. A - At. Mol. Opt. Phys.* **2006**, *73*, 062723.
- 1223 [12] Hubbell, J. H. *Phys. Med. Biol.* **1999**, *44*, R1.
- 1224 [13] Stepanek, J.; Blattmann, H.; Laissue, J. A.; Lyubimova, N.; Di Michiel, M.;
1225 Slatkin, D. N. *Med. Phys.* **2000**, *27*, 1664.
- 1226 [14] Horsley, J. A.; Stöhr, J.; Hitchcock, A. P.; Newbury, D. C.; Johnson, A. L.; Sette, F.
1227 *J. Chem. Phys.* **1985**, *83*, 6099.
- 1228 [15] Piancastelli, M. N.; Lindle, D. W.; Ferrett, T. A.; Shirley, D. A. *J. Chem. Phys.* **1987**,
1229 *86*, 2765.
- 1230 [16] Sheehy, J. A.; Gil, T. J.; Winstead, C. L.; Farren, R. E.; Langhoff, P. W. *J. Chem.*
1231 *Phys.* **1989**, *91*, 1796.
- 1232 [17] Cassuto, A.; Mane, M.; Jupille, J. *Surf. Sci. Lett.* **1991**, *249*, 8.
- 1233 [18] Tonner, B. P.; Kao, C. M.; Plummer, E. W.; Caves, T. C.; Messmer, R. P.; Sala-
1234 neck, W. R. *Phys. Rev. Lett.* **1983**, *51*, 1378.
- 1235 [19] Stöhr, J.; Outka, D. A.; Baberschke, K.; Arvanitis, D.; Horsley, J. A. *Phys. Rev. B*
1236 **1987**, *36*, 2976.
- 1237 [20] Solomon, J. L.; Madix, R. J.; Stöhr, J. *J. Chem. Phys.* **1988**, *89*, 5316.
- 1238 [21] Liu, A. C.; Stöhr, J.; Friend, C. M.; Madix, R. J. *Surf. Sci.* **1990**, *235*, 107.
- 1239 [22] Gasaneo, G.; Ancarani, L. U.; Mitnik, D. M.; Randazzo, J. M.; Frapiccini, A. L.;
1240 Colavecchia, F. D. *Adv. Quantum Chem.* **2013**, *67*, 153.
- 1241 [23] Mitnik, D. M.; Colavecchia, F. D.; Gasaneo, G.; Randazzo, J. M. *Comp. Phys. Comm.*
1242 **2011**, *182*, 1145.
- 1243 [24] Ambrosio, M. J.; Colavecchia, F. D.; Gasaneo, G.; Mitnik, D. M.; Ancarani, L. U. *J.*
1244 *Phys. B: At. Mol. Opt. Phys.* **2015**, *48*, 055204.
- 1245 [25] Messiah, A. *Quantum Mechanics*; North-Holland: Amsterdam, 1972.
- 1246 [26] Sanz-Vicario, J.; Bachau, H.; Martín, F. *Phys. Rev. A* **2006**, *73*, 033410.
- 1247 [26] Pérez-Torres, J. F.; Morales, F.; Sanz-Vicario, J. L.; Martín, F. *Phys. Rev. A* **2009**,
1248 *80*, 011402.
- 1249 [27] Sansone, G. *et al. Nature* **2010**, *465*, 763.
- 1250 [28] Fernández, J.; Martín, F. *New J. Phys.* **2009**, *11*, 043020.
- 1251 [29] Chandra, N. J. *Phys. B: At. Mol. Phys.* **1987**, *20*, 3405.
- 1252 [30] Edmonds, A. R. *Angular Momentum in Quantum Mechanics*; Princeton University
1253 Press: Princeton, 1957.
- 1254 [31] Chung, Y. M.; Lee, E.-M.; Masuoka, T.; Samson, J. A. R. *J. Chem. Phys.* **1993**, *99*,
1255 885.
- 1256 [32] Kelly, H. P. *Chem. Phys. Lett.* **1973**, *20*, 547.
- 1257 [33] Sanz-Vicario, J.; Palacios, A.; Cardona, J.; Bachau, H.; Martín, F. *J. Electron*
1258 *Spectros. Relat. Phenomena* **2007**, *161*, 182.
- 1259 [34] Hilton, P. R.; Nordholm, S.; Hush, N. S. *J. Electron Spectros. Relat. Phenomena* **1980**,
1260 *18*, 101.
- 1261 [35] Martin, P. H. S.; Rescigno, T. N.; McKoy, V.; Henneker, W. H. *Chem. Phys. Lett.*
1262 **1974**, *29*, 496.
- 1263 [36] Raseev, G. *J. Phys. B: At. Mol. Phys.* **1985**, *18*, 423.
- 1264 [37] Plummer, E. W.; Gustafsson, T.; Gudat, W.; Eastman, D. E. *Phys. Rev. A* **1977**,
1265 *15*, 2339.
- 1266 [38] Stratmann, R. E.; Bandarage, G.; Lucchese, R. R. *Phys. Rev. A* **1995**, *51*, 3756.
- 1267 [39] Levine, Z. H.; Soven, P. *Phys. Rev. A* **1984**, *29*, 625.
- 1268 [40] Davenport, J. *Phys. Rev. Lett.* **1976**, *36*, 945.
- 1269 [41] Stener, M.; Decleva, P.; Lisini, A. *J. Electron Spectrosc. Relat. Phenom.* **1995**, *74*, 29.
- 1270 [42] Lucchese, R.; Raseev, G.; McKoy, V. *Phys. Rev. A* **1982**, *25*, 2572.
- 1271 [43] Brion, C.; Tan, K. *Chem. Phys.* **1978**, *34*, 141.
- 1272 [44] Kilcoyne, D. A. L.; Nordholm, S.; Hush, N. S. *Chem. Phys.* **1986**, *107*, 225.
- 1273 [45] Lucchese, R.; McKoy, V. *Phys. Rev. A* **1982**, *26*, 1406.
- 1274 [46] Harvey, A. G.; Brambila, D. S.; Morales, F.; Smirnova, O. *J. Phys. B: At. Mol. Opt.*

- 1275 *Phys.* **2014**, *47*, 215005.
- 1276 [47] Carlson, T. A.; Gerard, P.; Krause, M. O.; Grimm, F. A.; Pullen, B. P. *J. Chem.*
1277 *Phys.* **1987**, *86*, 6918.
- 1278 [48] Venuti, M.; Stener, M.; Decleva, P. *Chem. Phys.* **1998**, *234*, 95.
- 1279 [49] Stener, M.; Fronzoni, G.; Decleva, P. *J. Chem. Phys.* **2005**, *122*, 234301.
- 1280 [50] Kilcoyne, D. A. L.; Nordholm, S.; Hush, N. S. *Chem. Phys.* **1986**, *107*, 255.
- 1281 [51] Wilhelmy, I.; Ackermann, L.; Gorling, A.; Roösch, N. *J. Chem. Phys.* **1994**, *100*,
1282 2808.
- 1283 [52] Langhoff, P. W. Aspects of Electronic Configuration Interaction in Molecular Photoion-
1284 ization. In *Electron-Atom and Electron-Molecule Collisions*; Hinze, J., Ed.; Springer:
1285 New York, 1983.
- 1286 [53] Daasch, W. R.; Davidson, E. R.; Hazi, A. U. *J. Chem. Phys.* **1982**, *76*, 6031.
- 1287 [54] van Dishoeck, E. F.; van Hemert, M. C.; Dalgarno, A. *J. Chem. Phys.* **1982**, *77*, 3693.
- 1288 [55] Decleva, P.; De Alti, G.; Lisini, A. *J. Chem. Phys.* **1988**, *89*, 367.
- 1289 [56] Bachau, H.; Cormier, E.; Decleva, P.; Hansen, J. E.; Martín, F. *Rep. Prog. Phys.*
1290 **2001**, *64*, 1815.
- 1291 [57] Apalategui, A.; Saenz, A. *J. Phys. B: At. Mol. Opt. Phys.* **2002**, *35*, 1909.
- 1292 [58] Vanne, Y. V.; Saenz, A. *J. Phys. B: At. Mol. Opt. Phys.* **2004**, *37*, 4101.
- 1293 [59] Fojón, O. A.; Fernández, J.; Palacios, A.; Rivarola, R. D.; Martín, F. *J. Phys. B: At.*
1294 *Mol. Opt. Phys.* **2004**, *37*, 3035.
- 1295 [60] Doweck, D.; Pérez-Torres, J. F.; Picard, Y. J.; Billaud, P.; Elkharrat, C.; Houver, J. C.;
1296 Sanz-Vicario, J. L.; Martín, F. *Phys. Rev. Lett.* **2010**, *104*, 233003.
- 1297 [61] Klamroth, T. *Phys. Rev. B* **2003**, *68*, 245421.
- 1298 Rohringer, N.; Gordon, A.; Santra, R. *Phys. Rev. A* **2006**, *74*, 043420.
- 1299 Schlegel, H. B.; Smith, S. M.; Li, X. *J. Chem. Phys.* **2007**, *126*, 244110.
- 1300 [62] Klinkusch, S.; Saalfrank, P.; Klamroth, T. *J. Chem. Phys.* **2009**, *131*, 114304.
- 1301 [63] Sonk, J. A.; Schlegel, H. B. *J. Phys. Chem. A* **2011**, *115*, 11832.
- 1302 [64] Nesbet, R. K. *Variational Methods in Electron-Atom Scattering Theory*; Plenum: New
1303 York, 1979.
- 1304 [65] Stratmann, R. E.; Lucchese, R. R. *J. Chem. Phys.* **1995**, *102*, 8493.
- 1305 [66] Dalgarno, A. *Proc. Phys. Soc. Sect. A* **1952**, *65*, 663.
- 1306 [67] Schirmer, J.; Cederbaum, L.; Domcke, W.; von Niessen, W. *Chem. Phys.* **1977**, *26*,
1307 149.
- 1308 [68] Larkins, F. P.; Richards, J. A. *Aust. J. Phys.* **1986**, *39*, 809.
- 1309 [69] Saito, N. *et al. J. Phys. B: At. Mol. Opt. Phys.* **2003**, *36*, L25.
- 1310 [70] Saito, N.; Toffoli, D.; Lucchese, R. R.; Nagoshi, M.; De Fanis, A.; Tamenori, Y.;
1311 Oura, M.; Yamaoka, H.; Kitajima, M.; Tanaka, H.; Hergenhahn, U.; Ueda, K. *Phys.*
1312 *Rev. A* **2004**, *70*, 062724.
- 1313 [71] Semenov, S. K.; Cherepkov, N. A.; Jahnke, T.; Dörner, R. *J. Phys. B: At. Mol. Opt.*
1314 *Phys.* **2004**, *37*, 1331.
- 1315 [72] Ågren, H.; Carravetta, V.; Vahtras, O.; Pettersson, L. G. M. *Theor. Chem. Acc.* **1997**,
1316 *97*, 14.
- 1317 [73] Nest, M.; Klamroth, T.; Saalfrank, P. *J. Chem. Phys.* **2005**, *122*, 124102.
- 1318 [74] Alon, O. E.; Streltsov, A. I.; Cederbaum, L. S. *Phys. Rev. A* **2009**, *79*, 022503.
- 1319 [75] Kato, T.; Kono, H. *J. Chem. Phys.* **2008**, *128*, 184102.
- 1320 [76] Haxton, D. J.; Lawler, K. V.; McCurdy, C. W. *Phys. Rev. A* **2011**, *83*, 063416.
- 1321 [77] Haxton, D. J.; Lawler, K. V.; McCurdy, C. W. *Phys. Rev. A* **2012**, *86*, 013406.
- 1322 [78] Hohenberg, P.; Kohn, W. *Phys. Rev.* **1964**, *136*, B864.
- 1323 [79] Kohn, W.; Sham, L. J. *Phys. Rev.* **1965**, *140*, A1133.
- 1324 [80] van Leeuwen, R.; Baerends, E. J. *Phys. Rev. A* **1994**, *49*, 2421.
- 1325 [81] Görling, A. *Phys. Rev. Lett.* **1999**, *83*, 5459.
- 1326 [82] Stener, M.; Decleva, P. *J. Electron Spectros. Relat. Phenomena* **1998**, *94*, 195.
- 1327 [83] Stener, M.; Decleva, P. *J. Electron Spectros. Relat. Phenomena* **1999**, *104*, 135.
- 1328 [84] Toffoli, D.; Stener, M.; Fronzoni, G.; Decleva, P. *Chem. Phys.* **2002**, *276*, 25.
- 1329 [85] Woon, D. E.; Park, J. *Astrophys. J.* **2004**, *607*, 342.
- 1330 [86] Stranges, S.; Turchini, S.; Alagia, M.; Alberti, G.; Contini, G.; Decleva, P.; Fron-
1331 zoni, G.; Stener, M.; Zema, N.; Prosperi, T. *J. Chem. Phys.* **2005**, *122*, 244303.
- 1332 [87] Toffoli, D.; Decleva, P.; Gianturco, F. A.; Lucchese, R. R. *J. Chem. Phys.* **2007**, *127*,
1333 234317.
- 1334 [88] Runge, E.; Gross, E. K. U. *Phys. Rev. Lett.* **1984**, *52*, 997.
- 1335 [89] Stener, M.; Decleva, P. *J. Chem. Phys.* **2000**, *112*, 10871.
- 1336 [90] Zangwill, A.; Soven, P. *Phys. Rev. A* **1980**, *21*, 1561.

- 1337 [91] Stener, M.; Fronzoni, G.; Toffoli, D.; Decleva, P. *Chem. Phys.* **2002**, *282*, 337.
- 1338 [92] Stener, M.; Decleva, P.; Cacelli, I.; Moccia, R.; Montuoro, R. *Chem. Phys.* **2001**,
- 1339 *272*, 15.
- 1340 [93] Stener, M. *Chem. Phys. Lett.* **2002**, *356*, 153.
- 1341 [94] Fronzoni, G.; Stener, M.; Decleva, P. *Chem. Phys.* **2004**, *298*, 141.
- 1342 [95] Toffoli, D.; Stener, M.; Fronzoni, G.; Decleva, P. *J. Chem. Phys.* **2006**, *124*, 214313.
- 1343 [96] Patanen, M.; Kooser, K.; Argenti, L.; Ayuso, D.; Kimura, M.; Mondal, S.; Plésiat, E.;
- 1344 Palacios, A.; Sakai, K.; Travnikova, O.; Decleva, P.; Kukk, E.; Miron, C.; Ueda, K.;
- 1345 Martín, F. *J. Phys. B: At. Mol. Opt. Phys.* **2014**, *47*, 124032.
- 1346 [97] Holland, D. M. P.; Potts, A. W.; Karlsson, L.; Stener, M.; Decleva, P. *Chem. Phys.*
- 1347 **2011**, *390*, 25.
- 1348 [98] Russakoff, A.; Bubin, S.; Xie, X.; Erattupuzha, S.; Kitzler, M. *Phys. Rev. A* **2015**,
- 1349 *91*, 023422.
- 1350 [99] Madjet, M. E.; Chakraborty, H. S.; Rost, J. M.; Manson, S. T. *J. Phys. B: At. Mol.*
- 1351 *Opt. Phys.* **2008**, *41*, 105101.
- 1352 [100] Stener, M.; Toffoli, D.; Fronzoni, G.; Decleva, P. *Theor. Chem. Acc.* **2007**, *117*, 943.
- 1353 [101] Plésiat, E.; Decleva, P.; Martín, F. *J. Phys. B: At. Mol. Opt. Phys.* **2012**, *45*, 194008.
- 1354 [102] Kukk, E. *et al. Phys. Rev. A* **2013**, *88*, 033412.
- 1355 [103] Reinhardt, W. P. *Ann. Rev. Phys. Chem.* **1982**, *33*, 223.
- 1356 [104] Moiseyev, N. *Phys. Rep.* **1998**, *302*, 212.
- 1357 [105] Nicolaides, C. A.; Beck, D. R. *Phys. Lett. A* **1978**, *65*, 11.
- 1358 [106] Simon, B. *Phys. Lett. A* **1979**, *71*, 211.
- 1359 [107] McCurdy, C. W.; Martín, F. *J. Phys. B: At. Mol. Opt. Phys.* **2004**, *37*, 917.
- 1360 [108] McCurdy, C. W.; Rescigno, T. N. *Phys. Rev. A* **1980**, *21*, 1499.
- 1361 [109] Rescigno, T. N.; McCurdy, C. W. *Phys. Rev. A* **1985**, *31*, 624.
- 1362 [110] Vanroose, W.; Martín, F.; Rescigno, T. N.; McCurdy, C. W. *Phys. Rev. A* **2004**, *70*,
- 1363 [111] Vanroose, W.; Horner, D. A.; Martín, F.; Rescigno, T. N.; McCurdy, C. W. *Phys.*
- 1364 *Rev. A* **2006**, *74*, 052702.
- 1365 [112] Rescigno, T. N.; Vanroose, W.; Horner, D. A.; Martín, F.; McCurdy, C. W. *J. Electron*
- 1366 *Spectros. Relat. Phenomena* **2007**, *161*, 85.
- 1367 [113] Light, J. C.; Hamilton, I. P.; Lill, J. V. *J. Chem. Phys.* **1985**, *82*, 1400.
- 1368 [114] Tao, L.; McCurdy, C. W.; Rescigno, T. N. *Phys. Rev. A* **2009**, *79*, 012719.
- 1369 [115] Tao, L.; McCurdy, C. W.; Rescigno, T. N. *Phys. Rev. A* **2009**, *80*, 013402.
- 1370 [116] Tao, L.; McCurdy, C. W.; Rescigno, T. N. *Phys. Rev. A* **2010**, *82*, 023423.
- 1371 [117] Yu, C.-h.; Pitzer, R. M.; McCurdy, C. W. *Phys. Rev. A* **1985**, *32*, 2134.
- 1372 [118] Morita, M.; Yabushita, S. *J. Comput. Chem.* **2008**, *29*, 2471.
- 1373 [119] Collins, L. A.; Schneider, B. I. *Phys. Rev. A* **1981**, *24*, 2387.
- 1374 Schneider, B. I.; Collins, L. A. *Phys. Rev. A* **1981**, *24*, 1264.
- 1375 [120] Collins, L. A.; Schneider, B. I. 2. The Linear Algebraic Method for Electron-Molecule
- 1376 Collisions. In *Computational Methods for Electron-Molecule Collisions*; Huo, M. W.;
- 1377 Gianturco, F. A., Eds.; Springer: New York, 1995.
- 1378 [121] Collins, L.; Schneider, B. *Phys. Rev. A* **1984**, *29*, 1695.
- 1379 [122] Schneider, B. I.; Collins, L. a. *Phys. Rev. A* **1983**, *27*, 2847.
- 1380 [123] Agassi, D.; Gal, A. *Ann. Phys. (NY)* **1973**, *75*, 56.
- 1381 [124] Korryng, J. *Physica* **1947**, *13*, 392.
- 1382 Kohn, W.; Rostoker, N. *Phys. Rev.* **1954**, *94*, 1111.
- 1383 Morse, P. M. *Proc. Nat. Acad. Sci. U. S.* **1956**, *42*, 276.
- 1384 [125] Dill, D.; Dehmer, J. L. *J. Chem. Phys.* **1974**, *61*, 692.
- 1385 [126] Johnson, K. H. Scattered-Wave Theory of the Chemical Bond. In *Advances in Quantum*
- 1386 *Chemistry*, Vol. 7; Lödwinn, P. O., Ed.; Academic: NY, 1973.
- 1387 [127] Slater, J. C.; Johnson, K. H. *Phys. Rev. B* **1972**, *5*, 844.
- 1388 [128] Davenport, J. W. *Int. J. Quantum Chem.* **1977**, *12*, 89.
- 1389 [129] Dehmer, J. L.; Dill, D. *J. Chem. Phys.* **1976**, *65*, 5327–5334.
- 1390 [130] Grimm, F. A. *Chem. Phys.* **1983**, *81*, 315.
- 1391 [131] Grimm, F. A.; Carlson, T. A.; Dress, W. B.; Agron, P.; Thomson, J. O.; Daven-
- 1392 port, J. W. *J. Chem. Phys.* **1980**, *72*, 3041.
- 1393 [132] Rosi, M.; Sgamellotti, A.; Tarantelli, F.; Andreev, V. A.; Gofman, M.; Nefedov, V.
- 1394 *J. Electron Spectros. Relat. Phenomena* **1986**, *41*, 439.
- 1395 [133] Tse, J. S.; Liu, Z. F.; Bozek, J. D.; Bancroft, G. M. *Phys. Rev. A* **1989**, *39*, 1791.
- 1396 [134] Ishikawa, H.; Fujima, K.; Adachi, H.; Miyauchi, E.; Fujii, T. *J. Chem. Phys.* **1991**,
- 1397 *94*, 6740.
- 1398 [135] Powis, I. *Chem. Phys. Lett.* **1993**, *215*, 269.

- 1399 [136] Powis, I. *Chem. Phys.* **1995**, 201, 189.
1400 [137] Powis, I. *J. Chem. Phys.* **1997**, 106, 5013.
1401 [138] Jürgensen, A.; Cavell, R. G. *J. Electron Spectros. Relat. Phenomena* **2003**, 128, 245.
1402 [139] Ellison, F. O. *J. Chem. Phys.* **1974**, 61, 507.
1403 [140] Kaplan, I. G.; Markin, A. P. *Opt. Spectrosc.* **1968**, 24, 475.
1404 [141] Kaplan, I. G.; Markin, A. P. *Opt. Spectrosc.* **1968**, 25, 275.
1405 [142] Lohr, L. L.; Robin, M. B. *J. Am. Chem. Soc.* **1970**, 92, 7241.
1406 [143] Thiel, W.; Schweig, A. *Chem. Phys. Lett.* **1971**, 12, 49.
1407 [144] Schweig, A.; Thiel, W. *Chem. Phys. Lett.* **1973**, 21, 541.
1408 [145] Rabalais, J. W.; Debies, T. P.; Berkosky, J. L.; Huang, J. J.; Ellison, F. O. *J. Chem. Phys.* **1974**, 61, 516.
1410 [146] Dewar, M. J. S.; Komornicki, A.; Thiel, W.; Schweig, A. *Chem. Phys. Lett.* **1975**, 31, 286.
1411 [147] Huang, J. T. J.; Ellison, F. O. *Chem. Phys. Lett.* **1975**, 32, 196.
1412 [148] Beerlage, M. J. M.; Feil, D. *J. Electron Spectros. Relat. Phenomena* **1977**, 12, 161.
1413 [149] Schweig, A.; Thiel, W. *J. Electron Spectros. Relat. Phenomena* **1974**, 3, 27.
1414 [150] Hilton, P. R.; Nordholm, S.; Hush, N. S. *Chem. Phys.* **1976**, 15, 345.
1415 [151] Deleuze, M.; Pickup, B. T.; Delhalle, J. *Mol. Phys.* **1994**, 83, 655.
1416 [152] Hilton, P. R.; Nordholm, S.; Hush, N. S. *J. Chem. Phys.* **1977**, 67, 5213.
1417 [153] Kilcoyne, D. A. L.; McCarthy, C.; Nordholm, S.; Hush, N. S.; Hilton, P. R. *J. Electron Spectros. Relat. Phenomena* **1985**, 36, 153–185.
1420 [154] Hilton, P. R.; Nordholm, S.; Hush, N. S. *Chem. Phys. Lett.* **1979**, 64, 515.
1421 [155] Kilcoyne, D. A. L.; Nordholm, S.; Hush, N. S. *Chem. Phys.* **1986**, 107, 213.
1422 [156] Burke, P. G.; Berrington, K. A., Eds.; *Atomic and Molecular Processes, an R-Matrix Approach*; Institute of Physics Publishing: Bristol, 1993.
1423 [157] Bartschat, K. *Comput. Phys. Commun.* **1998**, 114, 168.
1424 [158] Schneider, B. I. 8. An R-Matrix Approach to Electron-Molecule Collisions. In *Computational Methods for Electron-Molecule Collisions*; Huo, M. W.; Gianturco, F. A., Eds.; Springer: New York, 1995.
1425 [159] Noble, C. J. 14. R-Matrix for Intermediate Energy Scattering and Photoionization. In *Computational Methods for Electron-Molecule Collisions*; Huo, M. W.; Gianturco, F. A., Eds.; Springer: New York, 1995.
1426 [160] Schneider, B. I.; LeDourneuf, M.; Burke, P. G. *J. Phys. B: At. Mol. Phys.* **1979**, 12, L365.
1427 [161] Burke, P. G.; Seaton, M. J. *J. Phys. B: At. Mol. Phys.* **1984**, 17, L683.
1428 [162] Seaton, M. J. *J. Phys. B: At. Mol. Phys.* **1985**, 18, 2111.
1429 [163] Seaton, M. J. *J. Phys. B: At. Mol. Phys.* **1986**, 19, 2601.
1430 [164] Tennyson, J.; Noble, C.; Burke, P. *Int. J. Quantum Chem.* **1986**, XXIX, 1033.
1431 [165] Tennyson, J. *J. Phys. B: At. Mol. Phys.* **1987**, 20, L375.
1432 [166] Joachain, C. J. *J. Mod. Opt.* **2007**, 54, 1859.
1433 [167] Burke, P. G.; Colgan, J.; Glass, D. H.; Higgins, K. *J. Phys. B: At. Mol. Opt. Phys.* **2000**, 33, 143.
1434 [168] Colgan, J.; Glass, D. H.; Higgins, K.; Burke, P. G. *J. Phys. B: At. Mol. Opt. Phys.* **2001**, 34, 2089.
1435 [169] Saenz, A. *Phys. Rev. A* **2003**, 67, 033409.
1436 [170] Tashiro, M. *J. Chem. Phys.* **2010**, 132, 134306.
1437 [171] Amusia, M. Y.; Cherepkov, N. A. *Case Stud. At. Phys.* **1975**, 5, 47.
1438 [172] Amusia, M. Y. Theory of Photoionization: VUV and Soft X-Ray Frequency Region. In *VUV and Soft X-Ray Photoionization*; Becker, U.; Shirley, D. A., Eds.; Plenum: NY, 1996.
1439 [173] Rowe, D. *Rev. Mod. Phys.* **1968**, 40, 153.
1440 [174] Yabushita, S.; McCurdy, C.; Rescigno, T. *Phys. Rev. A* **1987**, 36, 3146.
1441 [175] Semenov, S.; Cherepkov, N.; Fecher, G.; Schönhense, G. *Phys. Rev. A* **2000**, 61, 032704.
1442 [176] Semenov, S. K.; Cherepkov, N. A. *J. Phys. B: At. Mol. Opt. Phys.* **2003**, 36, 1409.
1443 [177] Schirmer, J.; Mertins, F. *J. Phys. B: At. Mol. Opt. Phys.* **1996**, 29, 3559.
1444 [178] Semenov, S. K.; Cherepkov, N. A. *Chem. Phys. Lett.* **1998**, 291, 375.
1445 [179] Lucchese, R.; Zurales, R. *Phys. Rev. A* **1991**, 44, 291.
1446 [180] Semenov, S.; Cherepkov, N. *Phys. Rev. A* **2002**, 66, 022708.
1447 [181] Montuoro, R.; Moccia, R. *Chem. Phys.* **2003**, 293, 281.
1448 [182] Cacelli, I.; Carravetta, V.; Moccia, R. *Chem. Phys.* **1994**, 184, 213.
1449 [183] Carmona-Novillo, E.; Moccia, R.; Spizzo, P. *Chem. Phys.* **1996**, 210, 435.

- 1461 [184] Yasuike, T.; Yabushita, S. *Chem. Phys. Lett.* **2000**, *316*, 257.
- 1462 [185] Cherepkov, N.; Semenov, S.; Hikosaka, Y.; Ito, K.; Motoki, S.; Yagishita, A. *Phys.*
1463 *Rev. Lett.* **2000**, *84*, 250.
- 1464 [186] Polozkov, R. G.; Ivanov, V. K.; Solov'yov, A. V. *J. Phys. B: At. Mol. Opt. Phys.*
1465 **2005**, *38*, 4341.
- 1466 [187] Ivanov, V. K.; Kashenock, G. Y.; Polozkov, R. G.; Solov'yov, A. V. *J. Phys. B: At.*
1467 *Mol. Opt. Phys.* **2001**, *34*, L669.
- 1468 [188] Cacelli, I.; Carravetta, V.; Moccia, R.; Rizzo, A. *J. Phys. Chem.* **1988**, *92*, 979.
- 1469 [189] Langhoff, P. W. *Chem. Phys. Lett.* **1973**, *22*, 60.
- 1470 [190] Langhoff, P. W. Stieltjes-Tchebycheff Moment-Tehory Approach to Molecular Photoion-
1471 ization Studies. In *Electron-Molecule and Photon-Molecule Collisions*; Rescigno, T.;
1472 McKoy, V.; Schneider, B., Eds.; Plenum: NY, 1979.
- 1473 [191] Shohat, J. A.; Tamarkin, J. D. *The Problem of Moments*; volume 1 of *Mathematical*
1474 *Surveys* American Mathematical Society: Providence, 1943.
- 1475 [192] Corcoran, C. T.; Langhoff, P. W. *J. Math. Phys.* **1977**, *18*, 651.
- 1476 [193] Rescigno, T. N.; Bender, C. F.; McKoy, B. V.; Langhoff, P. W. *J. Chem. Phys.* **1978**,
1477 *68*, 970.
- 1478 [194] Barsuhn, J.; Nesbet, R. K. *J. Chem. Phys.* **1978**, *68*, 2783.
- 1479 [195] ONeil, S. V.; Reinhardt, W. P. *J. Chem. Phys.* **1978**, *69*, 2126.
- 1480 [196] Williams, G. R. J.; Langhoff, P. W. *Chem. Phys. Lett.* **1979**, *60*, 201.
- 1481 [197] Delaney, J. J.; Saunders, V. R.; Hillier, I. H. *J. Phys. B: At. Mol. Phys.* **1981**, *14*,
1482 819.
- 1483 [198] Diercksen, G. H. F.; Kraemer, W. P.; Rescigno, T. N.; Bender, C. F.; Mckoy, B. V.;
1484 Langhoff, S. R.; Langhoff, P. W. *J. Chem. Phys.* **1982**, *76*, 1043.
- 1485 [199] Cacelli, I.; Moccia, R.; Carravetta, V. *Chem. Phys.* **1984**, *90*, 313.
- 1486 [200] Cacelli, I.; Carravetta, V.; Moccia, R. *J. Phys. B: At. Mol. Phys.* **1985**, *18*, 1375.
- 1487 [201] Cacelli, I.; Carravetta, V.; Moccia, R. *Mol. Phys.* **1986**, *59*, 385.
- 1488 [202] Cacelli, I.; Carravetta, V.; Moccia, R. *Chem. Phys.* **1988**, *120*, 51.
- 1489 [203] Görling, A.; Rösch, N. *J. Chem. Phys.* **1990**, *93*, 5563.
- 1490 [204] Orel, A. E.; Rescigno, T. N.; Mckoy, B. V.; Langhoff, P. W. *J. Chem. Phys.* **1980**,
1491 *72*, 1265.
- 1492 [205] Gokhberg, K.; Vysotskiy, V.; Cederbaum, L. S.; Storchi, L.; Tarantelli, F.; Aver-
1493 bukh, V. *J. Chem. Phys.* **2009**, *130*, 064104.
- 1494 [206] Kohn, W. *Phys. Rev.* **1948**, *74*, 1763.
- 1495 [207] Rescigno, T. N.; McCurdy, C. W.; Orel, A. E.; Lengsfeld III, B. H. 1. The Complex
1496 Kohn Variational Method. In *Computational Methods for Electron-Molecule Collisions*;
1497 Huo, M. W.; Gianturco, F. A., Eds.; Springer: New York, 1995.
- 1498 [208] McCurdy, C. W.; Rescigno, T. N. *Phys. Rev. A* **1989**, *39*, 4487.
- 1499 [209] Manolopoulos, D.; Wyatt, R. *Chem. Phys. Lett.* **1988**, *152*, 23.
- 1500 [210] Manolopoulos, D. E.; Wyatt, R. E.; Clary, D. C. *J. Chem. Soc. Faraday Trans.* **1990**,
1501 *86*, 1641.
- 1502 [211] Le Rouzo, H.; Raşeev, G. *Phys. Rev. A* **1984**, *29*, 1214.
- 1503 [212] Manolopoulos, D. E. Lobatto Shape Functions. In *Numerical Grid Methods and Their*
1504 *Application to Schrödinger's Equation*; Cerjan, C., Ed.; Springer: Netherlands, 1993.
- 1505 [213] Rösch, N.; Wilhelmy, I. *Chem. Phys. Lett.* **1992**, *189*, 499.
- 1506 [214] Wilhelmy, I.; Rösch, N. *Chem. Phys.* **1994**, *185*, 317–332.
- 1507 [215] Orel, A. E.; Rescigno, T. N. *Phys. Rev. A* **1990**, *41*, 1695.
- 1508 [216] Rescigno, T.; Lengsfeld, B.; McCurdy, C. *Phys. Rev. A* **1990**, *41*, 2462.
- 1509 [217] Lynch, D. L.; Schneider, B. I. *Phys. Rev. A* **1992**, *45*, 4494.
- 1510 [218] Nesbet, R. K. *Phys. Rev. A* **1981**, *24*, 2975.
- 1511 [219] Rescigno, T. N.; Lengsfeld, B. H.; Orel, A. E. *J. Chem. Phys.* **1993**, *99*, 5097.
- 1512 [220] Orel, A. E.; Rescigno, T. N. *Chem. Phys. Lett.* **1997**, *269*, 222.
- 1513 [221] Jose, J.; Lucchese, R. R.; Rescigno, T. N. *J. Chem. Phys.* **2014**, *140*, 204305.
- 1514 [222] Schwinger, J. *Phys. Rev.* **1947**, *72*, 738 see p. 742.
- 1515 [223] Lippmann, B. A.; Schwinger, J. *Phys. Rev.* **1950**, *79*, 469.
- 1516 [224] Huo, W. M. 15. The Schwinger Variational Method. In *Computational Methods for*
1517 *Electron-Molecule Collisions*; Huo, M. W.; Gianturco, F. A., Eds.; Springer: New
1518 York, 1995.
- 1519 [225] Taylor, J. R. *Scattering Theory: The Quantum Theory of Nonrelativistic Collisions*;
1520 Wiley: NY, 1972.
- 1521 [226] Lucchese, R. R.; McKoy, V. *J. Phys. B: At. Mol. Phys.* **1979**, *12*, L421.

- 1522 [227] Takatsuka, K.; McKoy, V. *Phys. Rev. A* **1981**, *24*, 2473.
1523 Takatsuka, K.; McKoy, V. *Phys. Rev. A* **1984**, *30*, 1734.
1524 [228] Watson, D. K.; McKoy, V. *Phys. Rev. A* **1979**, *20*, 1474.
1525 [229] Lucchese, R. R.; Watson, D. K.; McKoy, V. *Phys. Rev. A* **1980**, *22*, 421.
1526 [230] Lucchese, R.; McKoy, V. *Phys. Rev. A* **1981**, *24*, 770.
1527 Lucchese, R.; McKoy, V. *Phys. Rev. A* **1983**, *28*, 1382.
1528 [231] Lynch, D.; Lee, M.-T.; Lucchese, R. R.; McKoy, V. *J. Chem. Phys.* **1984**, *80*, 1907.
1529 [232] Natalense, A. P. P.; Lucchese, R. R. *J. Chem. Phys.* **1999**, *111*, 5344.
1530 [233] Natalense, A.; Bescansin, L.; Lucchese, R. *Phys. Rev. A* **2003**, *68*, 032701.
1531 [234] Machado, L. E.; Bescansin, L. M.; Lima, M. A. P.; Braunstein, M.; McKoy, V. *J. Chem. Phys.* **1990**, *92*, 2362.
1532 Machado, L. E.; Lee, M.-T.; Bescansin, L. M. *J. Chem. Phys.* **1999**, *110*, 7228.
1533 [235] Machado, A. M.; Masili, M. *J. Chem. Phys.* **2004**, *120*, 7505.
1534 [236] Stephens, J. A.; McKoy, V. *J. Chem. Phys.* **1988**, *88*, 1737.
1535 [237] Braunstein, M.; McKoy, V.; Machado, L. E.; Bescansin, L. M.; Lima, M. A. P. *J. Chem. Phys.* **1988**, *89*, 2998.
1536 [238] Wells, M.; Lucchese, R. R. *J. Chem. Phys.* **1999**, *110*, 6365.
1537 [239] Gianturco, F.; Lucchese, R. *Phys. Rev. A* **2001**, *64*, 032706.
1538 [240] Wiedmann, R. T.; White, M. G.; Wang, K.; McKoy, V. *J. Chem. Phys.* **1994**, *100*, 4738.
1539 [241] Horáček, J.; Sasakawa, T. *Phys. Rev. A* **1983**, *28*, 2151.
1540 [242] Horáček, J.; Sasakawa, T. *Phys. Rev. A* **1984**, *30*, 2274.
1541 [243] Lee, M. T.; Iga, I.; Fujimoto, M. M.; Lara, O. *J. Phys. B: At. Mol. Opt. Phys.* **1995**, *28*, L299.
1542 [244] Lee, M. T.; Iga, I.; Fujimoto, M. M.; Lara, O. *J. Phys. B: At. Mol. Opt. Phys.* **1995**, *28*, 3325.
1543 [245] Ribeiro, E. M. S.; Machado, L. E.; Lee, M.-T.; Bescansin, L. M. *Comput. Phys. Commun.* **2001**, *136*, 117.
1544 [246] Machado, A.; Fujimoto, M.; Taveira, A.; Bescansin, L.; Lee, M.-T. *Phys. Rev. A* **2001**, *63*, 032707.
1545 [247] Nascimento, E. M.; Ribeiro, E. M. S.; Bescansin, L. M.; Lee, M.-T.; Machado, L. E. *J. Phys. B: At. Mol. Opt. Phys.* **2003**, *36*, 3621.
1546 [248] Crank, J.; Nicolson, P. *Proc. Cambridge Philos. Soc.* **1947**, *43*, 50.
1547 [249] Goldberg, A.; Shore, B. W. *J. Phys. B: At. Mol. Phys.* **1978**, *11*, 3339.
1548 [250] Picón, A.; Bahabad, A.; Kapteyn, H. C.; Murnane, M. M.; Becker, A. *Phys. Rev. A* **2011**, *83*, 013414.
1549 [251] Yuan, K.-J.; Lu, H.; Bandrauk, A. *Phys. Rev. A* **2011**, *83*, 043418.
1550 [252] Silva, R. E. F.; Catoire, F.; Rivière, P.; Bachau, H.; Martín, F. *Phys. Rev. Lett.* **2013**, *110*, 113001.
1551 [253] Bian, X.-B. *Phys. Rev. A* **2014**, *90*, 033403.
1552 [254] Shull, H.; Löwdin, P.-O. *J. Chem. Phys.* **1959**, *30*, 617.
1553 [255] Goscinski, O. *Adv. Quantum Chem.* **2002**, *41*, 51 Preliminary research unpublished. Included as an appendix.
1554 [256] Aquilanti, V.; Cavalli, S.; Coletti, C.; Grossi, G. *Chem. Phys.* **1996**, *209*, 405.
1555 [257] Aquilanti, V.; Cavalli, S.; De Fazio, D. *J. Chem. Phys.* **1998**, *109*, 3792.
1556 [258] Avery, J.; Shim, R. *Int. J. Quantum Chem.* **2001**, *83*, 1.
1557 [259] Avery, J.; Avery, J. *J. Math. Chem.* **2003**, *33*, 145.
1558 [260] Rawitscher, G. *Phys. Rev. C* **1982**, *25*, 2196.
1559 [261] Rawitscher, G. *Phys. Rev. E* **2012**, *85*, 026701.
1560 [262] Ovchinnikov, S. Y.; Macek, J. H. *Phys. Rev. A* **1997**, *55*, 3605.
1561 [263] Macek, J. H.; Yu Ovchinnikov, S.; Gasaneo, G. *Phys. Rev. A* **2006**, *73*, 032704.
1562 [264] Fano, U.; Cooper, J. *Rev. Mod. Phys.* **1968**, *40*, 441.
1563 [265] Fernández-Menchero, L.; Otranto, S. *Phys. Rev. A* **2010**, *82*, 022712.
1564 [266] Fernández-Menchero, L.; Otranto, S. *J. Phys. B: At. Mol. Opt. Phys.* **2014**, *47*, 035205.
1565 [267] Granados-Castro, C. M.; Gómez, I. A.; Ancarani, L. U.; Gasaneo, G.; Mitnik, D. M. Submitted for publication, 2015.
1566 [268] Granados-Castro, C. M.; Ancarani, L. U.; Gasaneo, G.; Mitnik, D. M. *J. Phys.: Conf. Ser.* **2015**, *601*, 012009.
1567 [269] Harriman, J. *Phys. Rev.* **1956**, *101*, 594.
1568 [270] Granados-Castro, C. M.; Ancarani, L. U.; Gasaneo, G.; Mitnik, D. M. *Few-Body Syst.* **2014**, *55*, 1029.
1569 [271] Moccia, R. *J. Chem. Phys.* **1964**, *40*, 2186.

- 1584 [272] Moccia, R. *J. Chem. Phys.* **1964**, *40*, 2176.
1585 [273] Moccia, R. *J. Chem. Phys.* **1964**, *40*, 2164.
1586 [274] Banna, M. S.; McQuaide, B. H.; Malutzki, R.; Schmidt, V. *J. Chem. Phys.* **1986**, *84*,
1587 4739.
1588 [275] Brion, C.; Hamnett, A.; Wight, G.; Van der Wiel, M. *J. Electron Spectros. Relat.*
1589 *Phenomena* **1977**, *12*, 323.
1590 [276] Backx, C.; der Wiel, M. J. V. *J. Phys. B: At. Mol. Phys.* **1975**, *8*, 3020.
1591 [277] Randazzo, J. M.; Buezas, F.; Frapiccini, A. L.; Colavecchia, F. D.; Gasaneo, G. *Phys.*
1592 *Rev. A* **2011**, *84*, 052715.
1593 [278] Randazzo, J. M.; *et al.*, *Eur. J. Phys. D* **2015**, Submitted for publication.
1594 [279] Cacelli, I.; Moccia, R.; Rizzo, A. *J. Chem. Phys.* **1993**, *98*, 8742.